ASSESSING THE IMPACT OF URBAN EXPANSION ON LAND SURFACE TEMPERATURE USING GEOSPATIAL TOOLS: THE CASE STUDY IN BISHOFTU CITY, ETHIOPIA

Aweke Atlaw Mamo

A thesis Submitted to the Department of Architecture

College of Civil Engineering and Architecture

Presented in partial fulfillment of the requirement for the degree of Master of Science in Geoinformatics Engineering

Office of Graduate Studies

Adama Science and Technology University

May, 2025

Adama, Ethiopia

ASSESSIN THE IMPACT OF URBAN EXPANSION ON LAND SURFACE TEMPERATURE USING GEOSPATIAL TOOLS: THE CASE STUDY IN BISHOFTU CITY, ETHIOPIA

Aweke Atlaw Mamo

Advisor

Getachew Berhanemeskel (PhD)

A thesis Submitted to the Department of Architecture

College of Civil Engineering and Architecture

Presented in partial fulfillment of the requirement for the degree of Master of Science in Geoinformatics Engineering

Office of Graduate Studies

Adama Science and Technology University

May, 2025

Adama, Ethiopia

Approval Sheet

I/we, the advisors of the thesis entitled "Assessing the impact of urban expansion on land surface temperature using geospatial tools: the case study in Bishoftu city, Ethiopia." and developed by Aweke Atlaw Mamo hereby certify that the recommendation and suggestions made by the board of examiners are appropriately incorporated into the final version of the thesis.

Getachew Berhanemeskel (PhD)	____________________	______________________
Major Advisor	Signature	Date

We, the undersigned, members of the Board of Examiners of the thesis by Aweke Atlaw Mamo have read and evaluated the thesis entitled "Assessing the impact of urban expansion on land surface temperature using geospatial tools: the case study in Bishoftu city, Ethiopia" and examined the candidate during open defense. This is, therefore, to certify that the thesis is accepted for partial fulfillment of the requirement of the degree of Master of Science in Geoinformatics Engineering.

______________________	______________________	______________________
Chairperson	Signature	Date
______________________	______________________	______________________
Internal Examiner	Signature	Date
______________________	______________________	______________________
External Examiner	Signature	Date

Final approval and acceptance of the thesis is contingent upon submission of its final copy to the Office of Postgraduate Studies (OPGS) through the Department Graduate Council (DGC) and College Graduate Committee (CGC).

______________________	______________________	______________________
Department Head	Signature	Date
______________________	______________________	______________________
College Dean	Signature	Date
______________________	______________________	______________________
Office of Postgraduate Studies, Dean	Signature	Date

Declaration

I hereby declare that this Master Thesis entitled "Assessing the impact of urban expansion on land surface temperature using geospatial tools: the case study in Bishoftu city, Ethiopia." is my original work. That is, it has not been submitted for the award of any academic degree, diploma or certificate in any other university. All sources of materials that are used for this thesis have been duly acknowledged through citation.

Aweke Atlaw Mamo ______________________ ______________________

Name of student Signature Date

Recommendation

I/we, the advisor(s) of this thesis, hereby certify that I/we have read the revised version of the thesis entitled "Assessing the impact of urban expansion on land surface temperature using geospatial tools: the case study in Bishoftu city, Ethiopia." prepared under my/our guidance by Aweke Atlaw Mamo submitted in partial fulfillment of the requirements for the degree of Mater's of Science in Geoinformatics Engineering. Therefore, I/we recommend the submission of revised version of the thesis to the department following the applicable procedures.

Getachew Berhanemeskel (PhD)	____________________	______________________
Major Advisor	Signature	Date

ACKNOWLEDGMENT

First and foremost, I want to express my gratitude to the "Almighty GOD" for providing me with the invaluable opportunity, fortitude, patience, and trust necessary to successfully finish my thesis work. Many individuals and organizations deserve sincere gratitude for their invaluable contributions to this study, second only to "God." I want to sincerely thank and be indebted to my advisor, Getachew Berhanemeskel (PhD), who supported me from the start of the research to its completion, shared their time with me for insightful conversations, and provided me with their kind and helpful advice during this study. I am really grateful to the National Meteorology Agency and the Space Science and Geospatial Institute for providing me with the crucial data and information required to carry out this study. I want to express my sincere gratitude to my family and the SSGI employees, especially Dawit Desalegn and Tilahun Alemayehu for their constant encouragement and support. Their unwavering encouragement and acknowledgment have been immensely helpful. I owe a debt of gratitude to everyone who has changed my life, including my former teachers, friends, and classmates, as well as to everyone who has helped along the way. Without the assistance and efforts of these people and organizations, this thesis would not have been feasible. I sincerely appreciate all of their hard work and devotion.

Table of Contents

LIST OF TABLES I

LIST OF FIGURES II

ACRONYMS AND ABBREVIATIONS III

ABSTRACT IV

CHAPTER ONE 1

1 INTRODUCTION 1

1.1. Background of the study 1

1.2 Statement of the problem 2

1.3 Objective of the study 3

1.3.1 General objective 3

1.3.2 Specific objectives 3

1.4 Research questions 3

1.5 Significance of the study 4

1.6 Scope of the study 4

1.7 Organization of the thesis 5

CHAPTER TWO 6

2. LITERATURE REVIEW 6

2.1 Conceptual Literature 6

2.1.1 Definition of Terms 6

2.1.2 Concept of Urban Expansion 6

2.2 Theoretical Literature 7

2.2.1 Types of Urban Expansion 7

2.2.2 Factors Driving Urban Expansion 7

2.2.3 Consequences of Urban Expansion 8

2.2.4 Land Surface Temperature 8

2.2.5 Algorithms for Retrieving Land Surface Temperature 9

2.2.6 Normalized Difference Vegetation Index 9

2.2.7 Normalized Difference Built-Up Index 10

2.2.8 The Role of Remote Sensing and GIS 10

2.3 Empirical Literature 11

2.4 Research Gaps in Existing Literature 11

2.5 Conceptual Framework 12

CHAPTER THREE 13
3. MATERIALS AND METHODS 13
3.1 Description of the study area 13
3.1.1 Location 13
3.1.2 Population 14
3.1.3 Topography 15
3.1.4 Climate 16
3.2 Research Approach and Design 19
3.3 Dara Collection and Sources 20
3.3.1 Primary data 20
3.3.2 Field data 20
3.3.3 Secondary data 21
3.4 Data Analysis 24
3.4.1 Digital Image Preprocessing 24
3.4.2 Image Classification 25
3.4.3 Land Use Land Cover Change Detection 27
3.4.4 Land Surface Temperature Retrieval 27
CHAPTER FOUR 32
4. RESULT AND DISCUSSION 32
4.1. LULC Change of Bishoftu city in 1990, 2007 and 2024 32
4.1.1 Geographical extent and spatial distribution of LULC 35
4.1.2 Accuracy assessment 37
4.1.3 Settlement expansion during 1990–2024 38
4.2 Normalized Difference Vegetation Index Analysis in Bishoftu city (1990–2024) 40
4.2.1 Trends in Vegetation Cover Changes 40
4.2.2 Spatial Distribution of Vegetation Cover 41
4.2.3 Urbanization's Impact on the Loss of Vegetation 41
4.2.4 Urban Planning Strategies for Vegetation Conservation 42
4.3 Relationship between LULC and NDVI 44
4.4 Normalized Difference Built up Index (NDBI) Analysis in Bishoftu city (1990–2024) 46
4.4.1 LULC and the NDBI Relationship in Bishoftu City (1990–2024) 48
4.5 Spatiotemporal Distribution of Land Surface Temperature 49
4.5.1 Changes in LULC and their effects on LST 51

4.5.2 Urban Area Land Surface Temperature from 1990 to 2024 53
4.5.3 Relationship Between LST and NDVI 56
4.5.4 Relationship between LST & NDBI 59
4.5.5 Relationship between Urban Expansion and Urban LST 61
4.5.6 Validation of the result for land surface temperature 63
4.6 Discussion 64
4.6.1 LULC Changes in Bishoftu city 64
4.6.2 Changes in Vegetation Cover: NDVI Analysis 65
4.6.3 Expansion of Built-Up Areas: NDBI Analysis 65
4.6.4 Land Surface Temperature (LST) Trends 65
4.6.5 Implications of Findings 66
4.6.6 Study Limitations and Future Research Directions 66
5. CONCLUSION AND RECOMMENDATIONS 68
5.1 Conclusion 68
5.2 Summary 68
5.3 Recommendations 69
References 69
APPENDICES 79

List of Tables

Table 3.1: Data sets and descriptions 20

Table 3. 2: Secondary data source 21

Table 3.3: Software's used for the study 22

Table 3.4: Lists the kinds of LULC along with a description of each 26

Table 4.1 LULC area and change of study area in 1990, 2007, and 2024 33

Table 4.2: Accuracy Assessment Results of Classification for 1990, 2007, and 2024 37

Table 4.3 NDVI Values for Bishoftu City (1990–2024) 40

Table 4.4. Changes in Mean NDVI Values for Different LULC Classes in Bishoftu City (1990–2024) 44

Table 4.5: NDBI Values for Bishoftu City (1990–2024) 47

Table 4.6 LULC and NDBI Changes in Bishoftu City (1990–2024) 49

Table 4.7 Mean Temperature of 1990, 2007 and 2024 50

Table 4.8 Mean Temperature and Changes in Temperature (1990–2024) 53

Table 4.9 Urban Area Land Surface Temperature from 1990 to 2024 54

List of Figures

Fig 2.1: Conceptual Framework (own design) ... 12

Fig 3.1: Location map of the study area ... 14

Fig 3.2: Population of Bishoftu City ... 15

Fig 3.3: Elevation map of the study area ... 16

Fig 3.4: The average temperature of Bishoftu ... 17

Fig 3.5: Monthly average rainfall of Bishoftu ... 18

Fig 3.6: Annual rainfall of Bishoftu ... 19

Fig 3.7: Methodological flow chart of the study ... 23

Fig 4.1: LULC area and changes of the study ... 34

Fig 4.2: Maps showing the LULC of study area ... 35

Fig 4.3: LULC Change detection analysis of study area from 1990 to 2024 ... 37

Fig 4.4: The pattern of the settlement area's growth from 1990 to 2024 ... 39

Fig 4.5: Study area NDVI maps (1990, 2007, and 2024) ... 43

Fig 4.6: Relationships between LULC and NDVI in Bishoftu City (1990–2024) ... 46

Fig.4.7: NDBI Maps of Bishoftu City (1990, 2007, and 2024) ... 48

Fig 4.8: Spatial Distribution of LST in Bishoftu (1990–2024) ... 51

Fig 4.9: Compares the mean LST across the five different LULC zones in Bishoftu during the study period ... 53

Fig 4.10: Urban Area Land Surface Temperature from 1990 to 2024 ... 55

Fig 4.11: Mean LST of urban area between 1990 and 2024 ... 56

Fig 4.12: Correlation between LST and NDVI within 1990 ... 58

Fig 4.13: Correlation between LST and NDVI within 2007 ... 59

Fig 4.14: Correlation between LST and NDVI within 2022 ... 59

Fig 4.15: Relationship between Urban Expansion and LST ... 63

ACRONYMS AND ABBREVIATIONS

DEM	Digital Elevation Model
DN	Digital Number
ERDAS	Earth Resources Data Analysis System
ETM+	Enhanced Thematic Mapper Plus
GIS	Geographical Information System
LSE	Land Surface Emissivity
LST	Land Surface Temperature
LULC	Land Use Land Cover
NDVI	Normalized Difference Vegetation Index
NIR	Near Infrared Radiation
MODIS	Moderate Resolution Imaging Spectroradiometer
OLI	Operational Land Imager
RS	Remote Sensing
TM	Thematic Mapper
TIRS	Thermal Infrared Sensor
TOA	Top of Atmospheric
UHI	Urban Heat Island
USGS	United State Geological Survey
UTM	Universal Transverse Mercator
WGS	World Geodetic System

ABSTRACT

The expansion of urban areas represents one of the most prominent and irreversible transformations in land cover and land use in recent human history. This study aims to assess the impact of urban expansion on LST in Bishoftu city, Ethiopia. Multi-temporal Landsat data from 1990 to 2024 were utilized to analyze the city's LULC patterns and LST. The maximum likelihood algorithm of supervised classification was employed to generate LULC maps, and LST was derived using emissivity values and satellite data as input parameters.

The relationship between LST and spectral indices, including the NDVI and NDBI, was examined through regression analysis. The findings revealed significant urban expansion, marked by an increase in built-up areas and a decline in agricultural and barren lands. Specifically, agricultural land decreased from 484.17 km² in 1990 to 438.61 km² in 2024 due to urban encroachment. The built-up area increased substantially from 15.59 km² in 1990 to 69.90 km² in 2024. Additionally, the mean LST in the urban area rose from 25.08°C in 1990 to 40.41°C in 2024, highlighting a significant warming trend. The mean LST in the built-up area rose by approximately 13.76°C between 1990 and 2024.

The study also revealed an inverse correlation between LST and NDVI, while a positive correlation was observed between LST and NDBI. These findings underscore the need for urban planning strategies that incorporate green spaces and vegetation development to mitigate the urban heat island effect. Consequently, stakeholders in Bishoftu city, Central Ethiopia, should prioritize the planting of trees and the establishment of green areas to help counterbalance the rising temperatures induced by urbanization.

Keywords: Bishoftu city's land surface temperature (LST), land use and cover (LULC), normalized difference vegetation index (NDVI), normalized difference built-up index (NDBI), and urban expansion.

CHAPTER ONE

1 INTRODUCTION

1.1. Background of the study

Urban land expansion is one of the most rapid, irreversible forms of land use and cover change, significantly affecting ecological and social systems (Gao & O'Neill, 2020). Driven by economic development and industrialization, urbanization leads to higher population densities, increased built-up areas, and urban living changes (Mundhe & Jaybhaye, 2014). Urbanization patterns vary by region worldwide, with the Global South-especially Asian and African cities growing more quickly than the Global North (Kundu & Pandey, 2020). With estimates showing an increase in the urban population from 11.3% in 2010 to 20.2% by 2050, urbanization is particularly fast in Africa and is having an impact on social, political, and economic dynamics (Kassouri & Okunlola, 2022). Ethiopia's urban population is also growing rapidly, with a projected increase from 17.3% in 2012 to 42.3 million by 2037 (Alliance, 2015). Bishoftu, a city in Oromia, Ethiopia, has seen significant urban growth, with its urban area expanding by 22% annually between 1995 and 2019 (Bulti & Abebe, 2020). Urbanization in Bishoftu and similar cities alters environmental factors, including air quality, rainwater runoff, soil conditions, and ambient temperature (Chen et al., 2017). Land use changes, particularly the substitution of impermeable materials like asphalt for natural surfaces, are mostly to blame for the rise in urban surface temperatures. This phenomenon disturbs evapotranspiration, increases runoff, and boosts land surface temperatures (Singh et al., 2014; Ayanlade et al., 2021).

The rise in land surface temperature (LST) has wide-reaching environmental implications, including urban heat islands, climate change, and public health (Mo et al., 2021). As LST is influenced by factors such as land use type, urban geometry, and building materials, it is essential for understanding urban environmental conditions, evapotranspiration, and temperature fluctuations (Govind & Ramesh, 2019; Ibitoye et al., 2017). Remote sensing tools, such as satellite imagery, have proven invaluable in monitoring LST and land use/cover (LULC) changes over time (Sresto et al., 2022; Attri et al., 2015).

This study focuses on Bishoftu, one of Ethiopia's largest cities, to evaluate how urban expansion over a 28year period has influenced LST. The rapid growth of Bishoftu, particularly over the past two decades, provides an important case for understanding the impact of urbanization on land surface temperatures (Merga et al., 2021).

1.2 Statement of the problem

Urbanization is one of the most significant global phenomena, especially in developing countries like Ethiopia, where rapid urban growth is reshaping landscapes, ecosystems, and local climates. In recent decades, Ethiopia has experienced an unprecedented rate of urban expansion, driven by economic development, industrialization, and population growth (Terfa et al., 2019). This urban expansion has led to drastic changes in land use and cover (LULC), resulting in various environmental challenges, including the rise in land surface temperatures (LST), altered energy balances, and the exacerbation of urban heat islands (UHI). As cities grow, their physical landscapes comprising impervious surfaces like roads, buildings, and parking lots replace natural vegetation and soil, leading to an increase in surface temperatures and a reduction in evapotranspiration, which further contributes to warming (Grover & Singh, 2010; Ebrahimy et al., 2021).

The city of Bishoftu, located in Ethiopia's Oromia region, is experiencing rapid urban growth, driven by both population migration and economic development. While there has been some research on the relationships between LULC changes and LST in Ethiopian cities, the available studies have not fully addressed the variations in LST, NDVI (Normalized Difference Vegetation Index), and NDBI (Normalized Difference Built-Up Index) correlations over time. Additionally, there is a lack of research that validates LST data using advanced remote sensing techniques, which is crucial for ensuring the accuracy of findings. Most existing studies on LST and urban heat islands in Ethiopia focus on broader trends or specific events, without considering how these variables change over different periods. Furthermore, no comprehensive studies have been conducted in Bishoftu to assess how these relationships evolve over an extended timeframe. This gap in knowledge limits the ability of urban planners and policymakers to develop targeted, sustainable strategies for managing urban heat and improving environmental quality in rapidly growing urban areas.

One of the key gaps in current research is the lack of analysis of how LST, NDVI, and NDBI relationships change over time. Understanding these dynamics is essential for assessing the long-term impacts of urbanization on surface temperatures and land use land cover. Another critical gap is the failure to validate LST data before analysis. Several studies on LST in Ethiopian cities have not validated their data, which undermines the reliability of the findings and limits the formation of evidence-based policies. Validation of LST data using advanced remote sensing tools, such as MODIS (Moderate Resolution Imaging Spectroradiometer), is essential for ensuring the accuracy of studies on urban climate and environmental change.

Despite the rapid urbanization in Bishoftu, no comprehensive study has been conducted to evaluate the spatiotemporal changes in land use land cover and the relationships between LST, NDVI, and NDBI over an extended period. Most studies on urbanization in Ethiopia are limited in scope or focus on short timeframes, leaving a significant gap in understanding the long-term impacts of urban growth. This research aims to fill these gaps by conducting an analysis of LST, NDVI, and NDBI correlations over a 35-year period (1990–2024). By examining how these variables evolve over time, this research will offer crucial insights for urban planners and policymakers in Bishoftu and other rapidly growing cities in Ethiopia. The findings will contribute to more sustainable urban development strategies, helping to mitigate the negative effects of urban heat islands and improve overall environmental quality in these urban centers.

1.3 Objective of the study

1.3.1 General objective

The general objective of the study was to Assessing the impact of urban expansion on land surface temperature using geospatial tools in Bishoftu city, Ethiopia.

1.3.2 Specific objectives

The specific objectives of the study are:

1. To evaluate the changes in land use and land cover in Bishoftu city from 1990 to 2024.

2. To investigate the distribution of LST, NDVI, and NDB in the study period.

3. To establish a correlation between LST and NDVI and NDBI indicators.

4. To examine the impact of urban growth on the city's land surface temperature.

1.4 Research questions

1. How have land use and land cover changed in Bishoftu city from 1990 to 2024?

2. What is the distribution pattern of LST, NDVI and NDBI during the study period?

3. What is the nature of the relationship between Land Surface Temperature (LST), NDVI, and NDBI indicators in Bishoftu city?

4. How much urban growth influenced the land surface temperature in Bishoftu city?

1.5 Significance of the study

Analyzing the spatiotemporal characteristics of changes in urban land use/land cover (LULC) is essential for providing up-to-date information on the rates, patterns, and growth processes of urban expansion. Understanding LST is crucial for grasping urban climate dynamics and the effects of LULC decisions on urban microclimates. The findings from this study will be beneficial for professionals such as landscape architects, environmental engineers, and urban planners, serving as a reference for managing urban green spaces to mitigate urban heat island (UHI) effects and promote sustainable development. Furthermore, the results will inform stakeholders involved in decision-making processes related to urban and rural land management, natural resource management, and environmental conservation. This research also lays a foundation for further studies in similar or related fields.

1.6 Scope of the study

The scope of this study was centered on evaluating the impact of urban expansion on land surface temperature (LST) in Bishoftu City, Ethiopia, by analyzing spatial and temporal changes in the years 1990, 2007, and 2024. The study employed geospatial tools, including remote sensing and Geographic Information Systems (GIS), to assess land use and land cover (LULC) dynamics over these key years, providing a historical perspective on urban growth patterns. Satellite imagery was used to classify different land cover types such as built-up areas, vegetation, and water bodies, and to derive LST data for each period. The research aimed to identify how urban expansion contributed to variations in surface temperatures, with particular attention to the development of urban heat islands. Spatial analysis was conducted to map changes in land cover and temperature distribution, while statistical methods established correlations between urban growth and temperature increases. The scope also considered limitations related to data resolution, availability, and potential inconsistencies across different years. Ultimately, this study sought to generate insights into the environmental effects of urbanization in Bishoftu, providing recommendations for sustainable urban planning and heat mitigation strategies within the Ethiopian context.

1.7 Organization of the thesis

The thesis is organized into five chapters, each addressing a critical aspect of the research. Chapter one introduces the study, providing an overview of the background, statement of the problem, research objectives, research questions, significance, scope, and the overall structure of the thesis. This chapter sets the foundation for understanding the purpose and direction of the research.

Chapter Two offers a comprehensive literature review, exploring both theoretical and conceptual perspectives relevant to the research topic. It delves into previous studies and research findings, providing a context for the study and identifying gaps in existing knowledge.

Chapter Three details the research methodology, outlining the methods and materials employed to achieve the study's objectives. This chapter describes the approach to data collection, analysis, and the tools used in the study, ensuring transparency and reproducibility of the research process.

Chapter Four presents the results of the study, followed by an in-depth discussion of the findings. This chapter analyzes the data in relation to the research objectives, providing insights into the impact of urban expansion on land surface temperature in Bishoftu city.

Finally, Chapter Five concludes the thesis by summarizing the key findings and offering recommendations based on the outcomes of the research. It also highlights the implications of the study and suggests areas for future research, providing a comprehensive conclusion to the thesis.

CHAPTER TWO

2. LITERATURE REVIEW

2.1 Conceptual Literature

2.1.1 Definition of Terms

Land and Land Resources: These refer to the Earth's terrestrial surface, including its biosphere features just above or below the surface. This encompasses elements such as climate, soil types, topography, surface water bodies (lakes, rivers, marshes), groundwater, flora and fauna, human settlements, and the effects of human activities (e.g., terracing, water management, roads, and buildings) (Briassoulis, 2009).

Land Cover: This term refers to the physical layer visible on the Earth's surface, such as vegetation, urban structures, water bodies, bare soil, and other features (Di Gregorio, 2005).

Land Use: Refers to the activities and arrangements made by humans within specific land cover types, aimed at creating, altering, or sustaining them (Di Gregorio, 2005).

Spectral Index: A mathematical formula applied to image spectral bands on a pixel-by-pixel basis for analysis (Gianquinto et al., 2011).

Temperature: A measure of the hotness or coldness of an object (Martin Kline, 2004).

Urban: An area with high population density and developed infrastructure, often referred to as a built-up area or urban agglomeration (McMillen Smith, 2003).

2.1.2 Concept of Urban Expansion

Urban Expansion refers to the growth of built environments within settlements, primarily driven by industrialization and economic development (Jiang et al., 2021). It is one of the most rapid and irreversible forms of land cover and land use change, resulting in significant ecological and social transformations (Gao & O'Neill, 2020). As the human population has increased, communities have evolved from rural settlements to citys, with major cities experiencing rapid growth. While large urban centers offer opportunities for innovation and wealth, they also require more resilient infrastructure and services. Urban heat islands, air pollution, traffic jams, habitat destruction, green space loss, and overburdened infrastructure and resources are just a few of the detrimental effects that can result from unchecked urbanization (Ebrahimy et al., 2021).

2.2 Theoretical Literature

2.2.1 Types of Urban Expansion

Urban land use expansion can occur in five primary forms:

Infilling involves developing previously vacant or redeveloped areas, such as brownfields (e.g., former industrial sites or abandoned shopping centers). Extension refers to new developments adjacent to existing areas, extending infrastructure like roads and utilities. Linear Development follows transportation corridors, such as highways or subways, leveraging existing accessibility. Sprawl is characterized by scattered suburban development, with each developer utilizing available plots without considering the overall urban layout. Finally, Large-Scale Projects include major infrastructure developments like ports, airports, or industrial zones, which often require significant land and can stimulate nearby development (Camagni et al., 2002).

2.2.2 Factors Driving Urban Expansion

The equilibrium between births and deaths is what propels natural population growth. Higher pregnancy rates among young people, who frequently migrate to metropolitan areas in search of housing, work, or education, cause population growth to accelerate and create a need for new living arrangements as they settle down and provide for their families (Mouridi, 2019).

Migration also plays a significant role in urban population growth. People move to cities for better job prospects, education, housing, and to escape inadequate social infrastructure or economic hardships. Political, racial, economic, or religious conflicts often compel individuals to migrate to urban areas for safety and opportunity (Asadzade et al., 2022).

Industrialization has been a key driver of urbanization. The industrial revolution brought new production methods and job opportunities in manufacturing, while modern agriculture reduced rural employment, prompting workers to seek jobs in cities. The promise of better wages has led many from rural areas to urban industrial centers (Raihan et al., 2022).

Commercialization has historically fueled urban growth, with cities like Athens, Sparta, and Venice acting as major commercial centers. Today, continued trade and commerce in urban areas attract more traders and workers, further contributing to the expansion of cities and Citys (Ekpeyong, 2020).

2.2.3 Consequences of Urban Expansion

Increased Air Pollution: Urban expansion leads to more traffic from cars, buses, and trucks, significantly contributing to air pollution and smog. Fossil fuel-powered vehicles are a major source of pollutants, raising greenhouse gas emissions and particulates, which harm public health, wildlife, and ecosystems (Wang et al., 2020).

Increased Water Pollution: Urban sprawl increases water pollution through runoff from streets, parking lots, and construction sites, carrying contaminants like gasoline, chemicals, and pet waste into nearby water bodies such as rivers and lakes (Ren Sun, 2014).

Climate Change: Rapid urbanization alters land use and cover, affecting local climates. One major result is the urban heat island (UHI) effect, where cities experience higher temperatures than surrounding rural areas, intensifying heat and modifying local climatic conditions (Guo et al., 2022).

Health Degradation: As cities expand, reliance on cars promotes sedentary lifestyles, reducing physical activity and increasing obesity. This leads to higher risks of mortality, cardiovascular diseases, and certain cancers (Awadall et al., 2013).

Loss of Open Space and Wildlife Habitats: Urban growth encroaches on agricultural lands, parks, and open spaces, leading to the loss of over a million acres annually. The conversion of natural areas into urban infrastructure threatens ecosystems and wildlife, exacerbated by pollution (La et al., 2014).

2.2.4 Land Surface Temperature

LST refers to the temperature of the land's surface, distinct from air temperature since land heats up and cools down more quickly (NASA, 2010). It is measured by remote sensors and provides insights into surface conditions, aiding the understanding of issues like evapotranspiration, temperature variations, and urban environmental conditions (Taloor et al., 2021; Govind & Ramesh, 2019). LST is an important environmental parameter linked to climate change, urban heat islands, droughts, and public health (Mo et al., 2021). In urban areas, factors such as day length, seasons, winds, topography, land use, and building materials influence LST (Ibitoye et al., 2017). According to Singh et al. (2014), the substitution of concrete and asphalt for natural surfaces raises surface temperatures, decreases evapotranspiration, and speeds up runoff. Therefore, analyzing LST and land use changes is crucial for creating sustainable, comfortable urban environments.

2.2.5 Algorithms for Retrieving Land Surface Temperature

Remote sensing, particularly thermal data from satellites, is a key method for estimating LST over large areas. Geostationary satellites are especially effective in capturing the diurnal cycle of LST (Trigo et al., 2012). The relationship between satellite-based thermal infrared (TIR) data and LST is established through the radiative transfer equation. Interest in LST retrieval from TIR data dates back to the 1970s (Li et al., 2013). Over time, various methods and data sources, including ground-based and satellite datasets have been used to study urban LST changes. Landsat imagery, with its high spatial resolution in thermal bands, is commonly used to measure and analyze LST in urban areas (Yin et al., 2020).

Several algorithms are used to extract LST from satellite images, including the split-window method, single-channel algorithm, temperature/emissivity separation method, and mono-window algorithm (Ayanlade et al., 2021). The split-window algorithm (SWA) is the most widely used for LST retrieval. It compensates for atmospheric effects by utilizing the differential absorption of two adjacent TIR channels (around 11 and 12 μm), effectively calculating LST based on the varying atmospheric absorption in these bands (Mirsanjari et al., 2021; Wang et al., 2019).

2.2.6 Normalized Difference Vegetation Index

The NDVI is a key tool in remote sensing, widely used to assess vegetation by simplifying multi-spectral imagery (Huang et al., 2021). Urban green spaces and vegetation play a vital role in maintaining environmental quality and balancing human-environment interactions (Roza et al., 2017; Oliveira et al., 2011). Vegetation influences ground temperatures, with higher NDVI values typically linked to lower LST due to evapotranspiration, which transfers latent heat from the ground to the atmosphere. Areas with high NDVI often experience cooler LSTs (Li et al., 2013).

Research has shown that vegetation type, distribution patterns, and green cover density significantly contribute to reducing LST (Odindi et al., 2015; Sruthi & Mohammed, 2015). According to research, LST increased by 3–8°C in regions of Ethiopia with little vegetation between 1985 and 2015. All of Addis Ababa's sub-cities have shown a negative association between NDVI and LST (Gebrekidan et al., 2021). Additionally, studies by Balew and Korme (2020) demonstrate a positive correlation between LST and the NDBI, while highlighting a negative correlation with NDVI, reinforcing the strong inverse relationship between vegetation cover and land surface temperature (Chaithanya et al., 2017).

2.2.7 Normalized Difference Built-Up Index

When employing remote sensing data to map urban built-up areas, the NDBI is a useful tool. It helps identify the extent and density of impervious surfaces, such as asphalt roads, parking lots, and constructed areas (Zha et al., 2003; Malik et al., 2019). These surfaces reflect more light in the short-wave infrared spectrum compared to the near-infrared spectrum (Alhawiti and Mitsova, 2016). Short-wave and near-infrared bands from remote sensing data are used to compute the Normalized Different, which has values between -1 and +1. Whereas a lower value (around -1) shows the existence of vegetation or a lack of built-up surfaces, a higher NDBI value, approaching 1, indicates a greater presence of built-up areas. Nice A useful tool for mapping urban built-up areas using remote sensing data is the Built-Up Index (NDBI). The NDBI is a significant spectral index that shows a strong correlation with land surface temperature. The presence of artificial structures alters the balance between surface sensible heat flux and latent heat flux. Impervious surface area and NDBI, derived from satellite imagery, are often employed as indicators for characterizing land surface temperature (Yang et al., 2017).

2.2.8 The Role of Remote Sensing and GIS

Remote Sensing (RS) is the art, science, and technology of using instrument-based methods to observe objects, scenes, or events (Damen, 2022). It offers useful data for examining changes in large-scale environmental features throughout time and space. RS data is used in various civil and military applications, including perimeter reconnaissance, urban planning, radiation monitoring, land use monitoring, growth regulation, environmental damage assessment, agricultural yield estimation, and geographic mapping (Javed et al., 2021).

The part of RS called thermal remote sensing is concerned with gathering, analyzing, and interpreting data in the electromagnetic spectrum's thermal infrared (TIR) region. It plays a crucial role in estimating LST, with tools such as geometrically corrected Landsat TIR Band 6 and Landsat 8 TIR Bands 10 and 11 used to calculate surface temperatures (Khin et al., 2012).

A Geographic Information System (GIS), as defined by Coppin and Bauer (1996), is a system designed to collect, process, and store, evaluate, organize, and display spatial and geographic data. GIS data can be categorized into spatial (location-based) and non-spatial (tabular) data. According to Burrough (1990), GIS data consists of three dimensions: spatial, temporal, and attribute. The use of advanced GIS and remote sensing technologies to track spatiotemporal changes in LULC and surface temperature has become a growing area of research globally (Alemu, 2019).

2.3 Empirical Literature

Urban expansion is increasingly converting agricultural land for infrastructure, industry, and housing, leading to changes in land use and rising land surface temperatures (LST), which negatively affect urban ecology (Bao et al., 2016). Studies show a strong correlation between urbanization and LST changes. For instance, Wang et al. (2016) found that impermeable surfaces in Nanjing, China, displaced vegetation, worsening biodiversity loss and temperature changes. Similarly, Esteque et al. (2016) discovered that in Southeast Asian cities, impermeable surfaces had LSTs 3°C higher than green spaces, underscoring the cooling role of vegetation.

Bezela et al. (2018) observed in Belem, Brazil, that areas with less vegetation had higher LSTs (30-35°C), indicating urban temperature discomforts. Luo & Wu (2021) found that Taiyuan, China, experienced a 5.17°C increase in average surface temperature from 1990 to 2014, coinciding with a significant expansion of impervious surfaces. In Gujranwala, Pakistan, Liaqut et al. (2019) reported an 8°C rise in surface temperature due to urbanization, with a negative correlation between vegetation (NDVI) and LST, further emphasizing the cooling effect of green spaces.

2.4 Research Gaps in Existing Literature

Research gaps in existing literature the absence of seasonal analyses investigation the correlations between LST NDVI and NDBI represents a critical gap in the study of urban environments, particularly in Ethiopian cities. A methodological gap in current studies lies in the lack of strict validation of LST data prior to analysis.

Furthermore, despite the rapid urbanization occurring in Ethiopian there is a lack of comprehensive studies that assess spatiotemporal dynamics land use land cover change and their relationship with LST, NDVI &NDBI over extended periods. Most research on urbanization in Ethiopia is constrained by short temporal scopes or narrow regional focuses, leaving significant gaps in understanding the long-term impacts of urban growth. By utilizing validated MODIS remote sensing data, this research will provide a more accurate and reliable assessment of urban climate trends. The study's focus on temporal and seasonal variations aims to generate variable insights fir urban planners and policymakers, facilitating the development of sustainable urban growth strategies to mitigate the adverse effect of urban heat islands and enhance environmental quality and other rapidly urbanizing Ethiopian cities.

2.5 Conceptual Framework

In research, a theoretical structure is an image that can help in demonstrating the probable causal relationship. It is sometimes referred to as a research model or conceptual model. The model incorporates a variety of variables and the presumptive connections among them, reflecting the expectations. LST is highly dependent on different kinds of landforms.

The value of LST is increased by built-up areas, dry soil, rocks, metaled roads, and concrete infrastructure, while it is decreased by water, wetland, woodland, grassland, scrubland, and farmed land. For these many types of landscape formations, the degree of covering and health varies with the season.

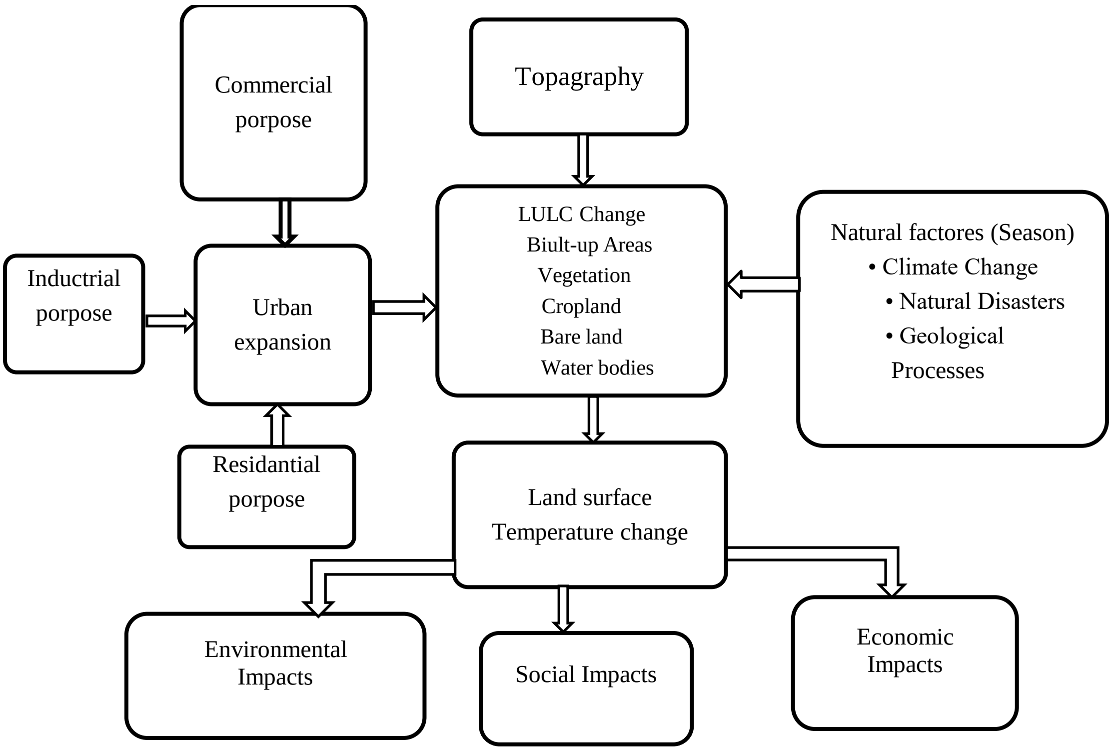

Fig 2.1: Conceptual Framework (own design)

CHAPTER THREE

3. MATERIALS AND METHODS

3.1 Description of the study area

3.1.1 Location

Bishoftu is a city located in the East Shewa Zone of the Oromia Region, situated approximately 50 km west of the zonal capital, Adama. Part of the Bishoftu volcanic area, this city is well-known for its collection of volcanic crater lakes. The city itself is characterized by a closed system, being encircled by steep and rocky hills and cliffs, typical of the volcanic crater lakes in the region. Geographically, Bishoftu is positioned at an astronomical location between the latitudes 8°39'20"−8°53'20"N and longitudes 38°48'15"−39°7'30"E, covering a total area of 542.65 km^2 (Fig 3.1). It lies 47.9 km southeast of Addis Ababa, along the Route 4 highway, and is a well-known resort city primarily due to its numerous lakes.

The city is located in a volcanic field that includes maars, cinder cones, tuff rings, and Holocene lava flows. Several of these maars are water-filled, giving rise to five distinct crater lakes: Lake Guda, Lake Koriftu, Lake Bishoftu, Lake Hora (a base for water sports, home to a variety of water birds, and the site of an annual festival), and the seasonal Lake Cheleklaka. Along with these lakes, Mount Yerer, Green Crater Lake, and Lake Hora Kiloli are other noteworthy geological and ecological phenomena in the area.

Because it is the location of Harar Meda Airport and the Ethiopian Air Force, Bishoftu is also a significant military and transportation hub. Additionally, it serves as a station on the Addis Ababa–Djibouti Railway, further enhancing its strategic and logistical significance.

The city of Bishoftu is located in Ethiopia's middle Rift Valley in Great East Africa. Kiremt (the rainy season), Bega (the dry period), Belg (the little rains), and Meher (the interval between the long and little rains) are the four distinct seasons of the climate. The hottest and coldest months in the city are May and December, respectively. June, July, August, and September are typically the rainy season, whereas January, October, November, and December are the driest months. December is the coldest or driest month of the year.

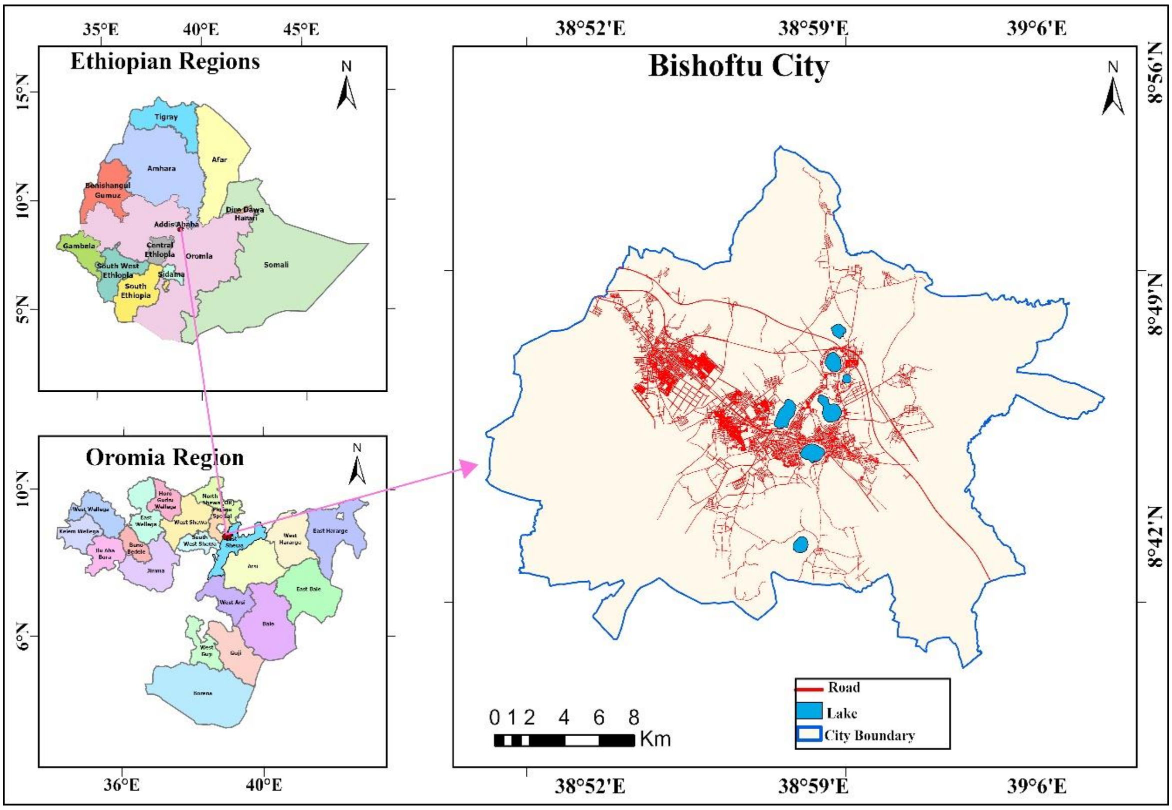

Fig 3.1: Location map of the study area

3.1.2 Population

As per the Central Statistical Agency (CSA) of Ethiopia's 2007 Population and Housing Census, there were 100,114 people living in Bishoftu city, with 47,225 men and 52,889 women. By 2016, the population was projected to grow significantly to 228,936 with 108,452 males and 120,484 females, all residing in urban areas. This represents a substantial increase of approximately 53.7% over less than a decade, underscoring Bishoftu’s rapid urban expansion and its increasing importance as a residential, economic, and administrative center of Oromia Region. The sharp population growth reflects the city’s development momentum and its rising significance within the regional urban landscape.

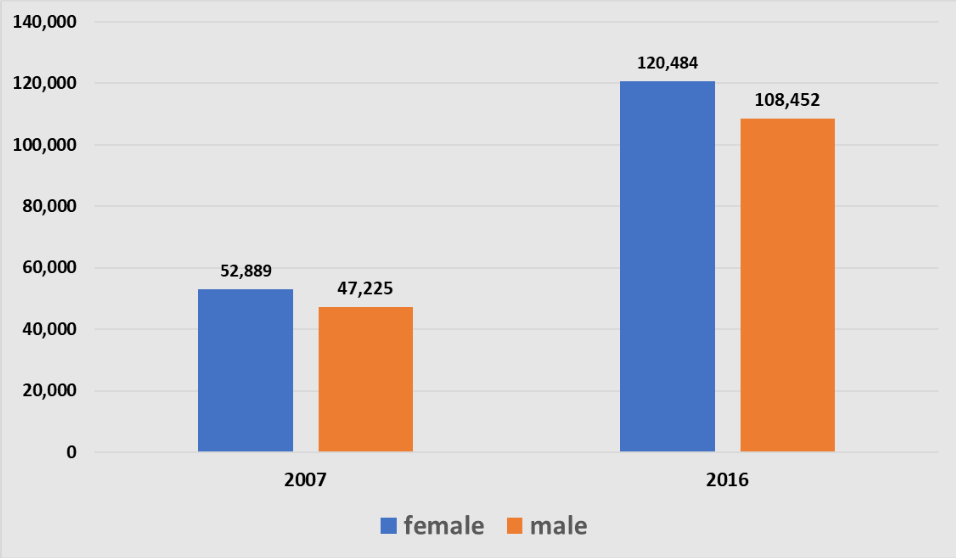

Fig 3.2: Population of Bishoftu city

3.1.3 Topography

The topography of Bishoftu is distinguished by a diverse landscape, including volcanic features, lakes, and varying elevations.

Volcanic Origin: Known for its volcanic origin, Bishoftu lies in the East African Rift System. The region exhibits characteristic volcanic hills and craters, which are remnants of ancient tectonic activity. As part of the Ethiopian Rift Valley, the area is geologically active, and its volcanic features are a significant aspect of its landscape.

Lakes: One of the many crater lakes in the area inspired the name of the city of Bishoftu. One of the most visible lakes in the city is Lake Bishoftu, sometimes referred to as Lake Debre Zeit. It is located within a caldera, formed by volcanic activity, and plays a central role in the city's natural environment and appeal.

Volcanic Hills and Craters: Surrounding Bishoftu is numerous volcanic hills and craters, remnants of past volcanic eruptions. These features contribute to the dramatic and unique scenery of the region, offering a distinct topographical character shaped by ancient volcanic processes.

Elevation Range: Bishoftu is situated at an altitude of approximately 1,815 meters above sea level. The northern and northwestern parts of the study area are characterized by higher elevations, reaching around 2,874 meters, as depicted in the elevation map (Figure 3.3). This variation in elevation significantly influences the city's climate, which is generally moderate, with mild temperatures throughout the year. The diverse topography also affects local weather patterns, further enhancing Bishoftu appeal as a popular resort destination.

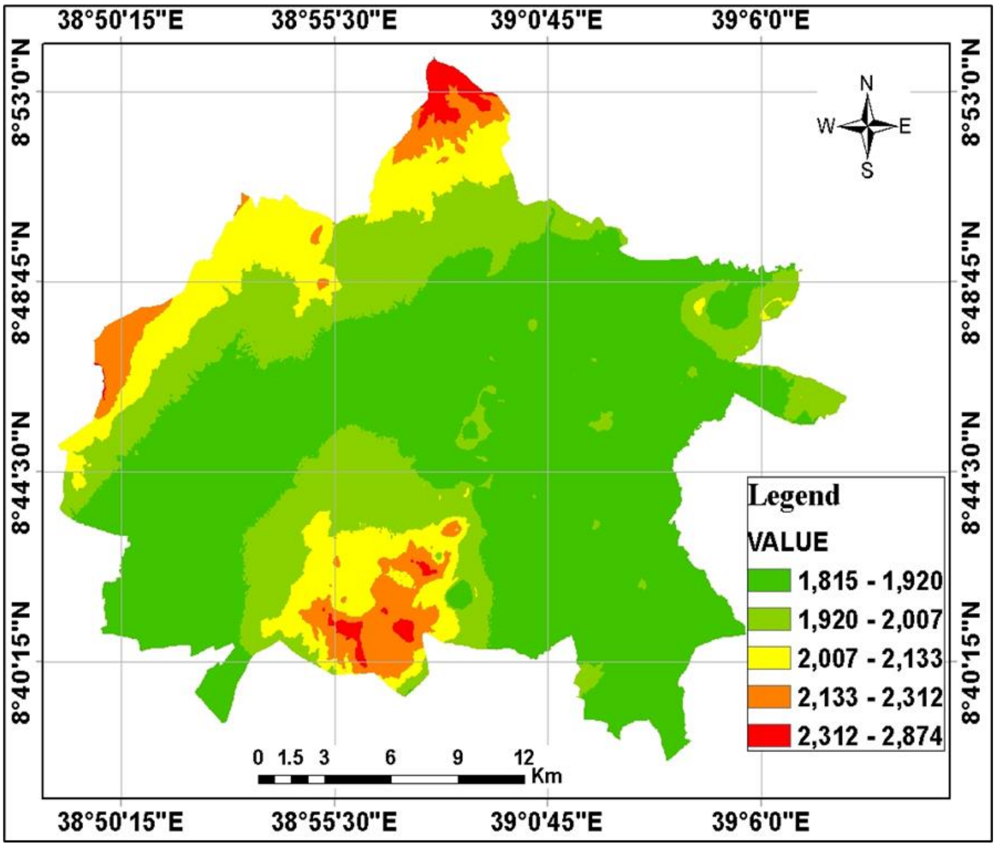

Fig 3.3: Elevation map of the study area

3.1.4 Climate

The climate of Bishoftu is classified as tropical highland climate under the Koppen-Geiger system, though it is also influenced by the city's altitude and its proximity to the East African Rift.

Temperature: Bishoftu, located at an altitude of approximately 1,900 meters (6,234 feet) above sea level, experiences a moderate climate throughout the year. The average temperature in the region typically ranges between 15°C and 25°C (59°F to 77°F), with noticeable diurnal temperature variation, where mornings and evenings tend to be cooler. Daytime temperatures can become warmer, particularly during the dry season, but extreme heat is rare. The climate was reflective of subtropical highland conditions, where the balance between daytime heat and cooler nights is maintained, contributing to the overall comfort of the area.

Monthly temperature data reveals a distinct seasonal pattern, with February being the hottest month, reaching a mean temperature of 30.9°C, followed by May at 30.3°C. In contrast, the cooler months of September and October exhibit mean temperatures of 21.3°C and 22.2°C, respectively. November also sees a reduction in temperature, averaging 23.5°C. Throughout the rest of year, temperatures remain relatively stable, with January and December both averaging 26.1°C and 26.4°C, respectively. The moderate nature of the temperature fluctuations, combined with the mild heat of the dry season, underscores Bishoftu's favorable climatic conditions, making it a notable example of subtropical highland climates in the region.

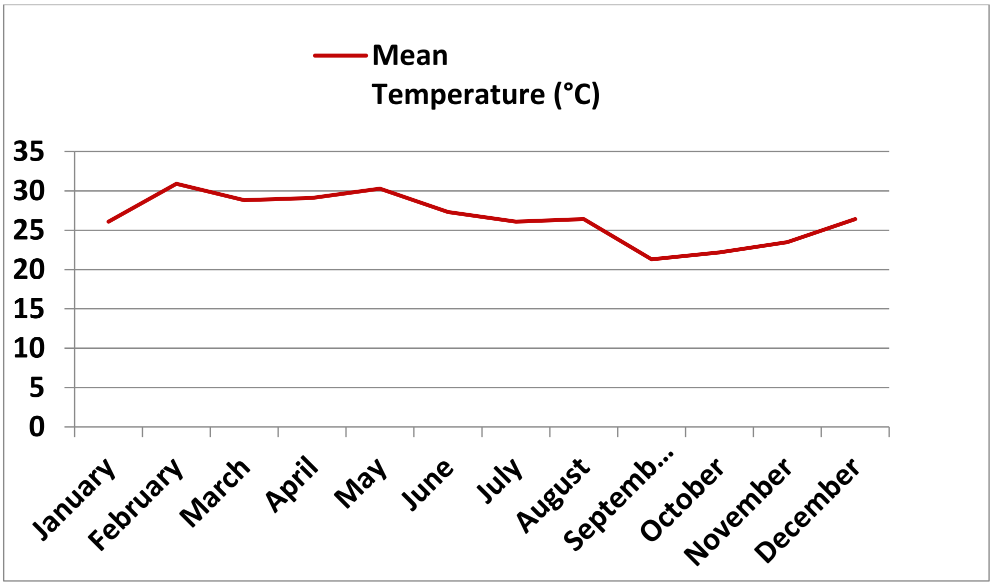

Fig 3.4: The average temperature of Bishoftu

Rainfall: The annual rainfall data for Bishoftu from 1990 to 2024 reveals a relatively stable rainfall pattern with moderate variability from year to year. The city's annual rainfall ranges from 860 to 950 mm, indicating a generally stable precipitation regime that is characteristic of areas impacted by the Inter-Tropical Convergence Zone (ITCZ). The highest recorded annual rainfall was 950 mm in both 2007 and 2012, while the lowest annual total was observed in 1994 and 2008, with 860 mm.

Throughout the 35-year period, annual rainfall values fluctuated within a narrow band, mostly ranging between 870 mm and 930 mm. The years 1990, 2005, 2014, and 2015 showed annual totals on the lower end of the spectrum (~860 mm to ~870 mm), while years such as 2007, 2012, and 2016 recorded rainfall near the 950 mm mark. This suggests that while the region generally experiences a consistent level of precipitation, specific years can see slight increases or decreases, potentially influenced by global climatic factors such as El Niño and La Niña events, which often affect East Africa's weather patterns.

The data also shows no significant trend of increasing or decreasing rainfall over the period from 1990 to 2024, indicating that the region's overall climate has remained relatively stable despite occasional anomalies. This stability is important for understanding long-term patterns and for planning in agriculture, water resource management, and infrastructure development in the region. In terms of annual averages, Bishoftu's precipitation has consistently supported its agricultural landscape, sustaining both crop and livestock farming, though variability still requires adaptive management strategies to cope with both excess and deficit rainfall years.

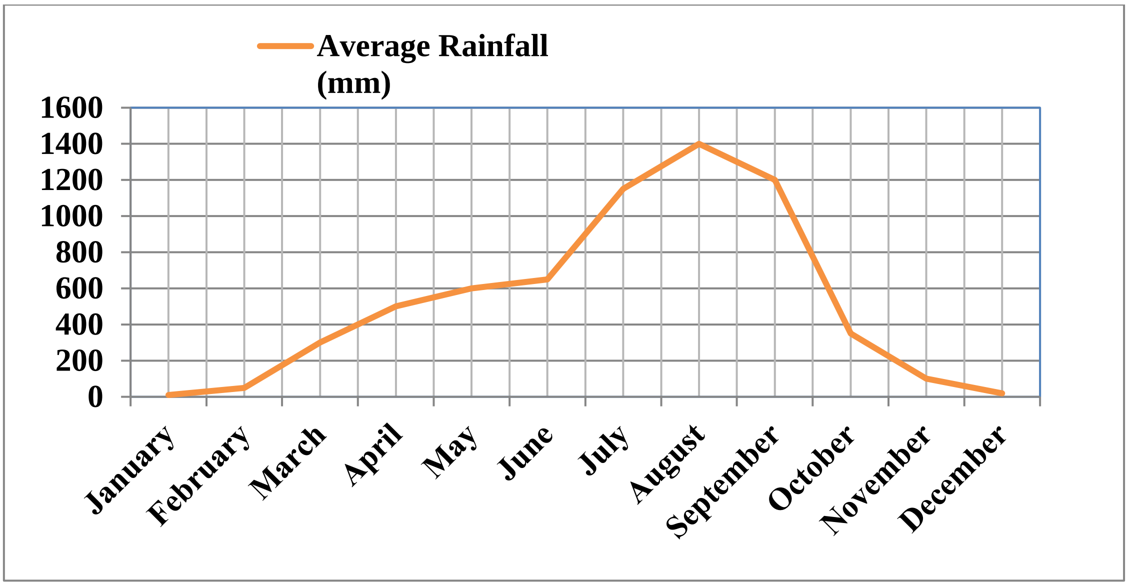

Fig 3.5: Monthly average rainfall of Bishoftu

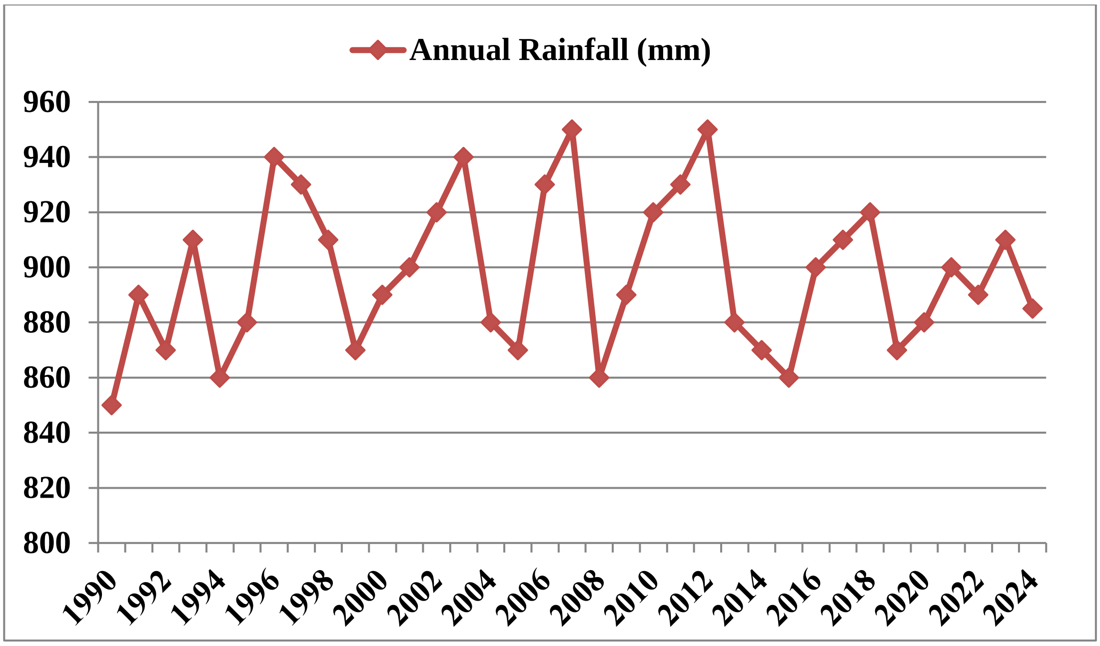

Fig 3.6: Annual rainfall of Bishoftu

Seasonal Variation: The climate is characterized by two primary seasons: the rainy season (belg and kiremt) and the dry season (bega and bega birra).

The temperatures remain relatively stable year-round, though it can be slightly cooler during the rainy months and warmer during the dry months.

Microclimates: Bishoftu's location to lakes (like Lake Bishoftu) and volcanic features may have an impact on the local microclimate, with higher humidity levels and temperature fluctuations brought on by elevation shifts.

3.2 Research Approach and Design

A mixed methods methodology was used for this study. This means the study's data collection and analysis employed a mix of methods from both quantitative and qualitative research approaches. Because it makes it possible to successfully meet the study's objectives, the mixed methods strategy is chosen for this investigation above the other research approaches.

However, the type of research approach to be employed defines the type of research design. Since the mixed methods technique is the recommended research methodology, the concurrent located model was the study's unique research design. In other words, data collection, analysis, and reporting were done using both quantitative and qualitative approaches concurrently or side by side.

3.3 Dara Collection and Sources

3.3.1 Primary data

Our study made use of the Landsat image obtained by Landsat 5 TM, Landsat 7 ETM+, and Landsat 8 OLI/TIRS, MODIS, and Ground truth. MODIS was obtained from https://earthdata.nasa.gov, whereas Landsat 5 and 8 were obtained from the USGS website (http://earthexplorer.usgs.gov). The sources of the data, their intended use, and thorough explanations are listed in Table 3.1

Table 3.1: Data sets and descriptions

S. No	Data Sets	Acquisitions Date	Source	Resolution Purpose	Purpose of the data
1	Landsat 5 TM	1990	USGS	30m	For LULC, LST, NDVI, NDBI
2	Landsat 7 ETM+	2007	USGS	30m	For LULC, LST, NDVI, NDBI
3	Landsat 8 OLI/TIRS	2024	USGS	30m	For LULC, LST, NDVI, NDBI
4	Ground truth	2024	GPS	2m	For LULC Validation
5	MODIS	2024	USGS	1Km	For LST Validation

3.3.2 Field data

This work used GPS data as field data to verify and evaluate the accuracy of LUCC-categorized images in different classes. After the random point creation, field GPS point collection and picture documentation displaying various LUCC classes were conducted. These field observations guaranteed the quality and dependability of the categorized photos by acting as ground truth for validation and accuracy evaluations.

3.3.3 Secondary data

Two examples of secondary data that were heavily used in the study are the average monthly temperature and the average monthly rainfall from 1990 to 2024. These datasets were essential for assessing and confirming the results. Additionally, the Ethiopian Geological Survey provided a geological map that provided important context for understanding the research area's geology. Furthermore, the CSA population data added vital demographic details that enhanced our comprehension of population dynamics within the purview of the study. The study was able to thoroughly examine the environmental, geological, and demographic elements influencing the study area by combining this disparate information, which allowed for reliable results and well-informed decision-making processes.

Secondary data source

Data description involves summarizing and presenting key characteristics of a dataset to facilitate understanding and analysis. At the same time, source refers to the origin or the place from which the data was obtained, providing important context for its interpretation and use. Table 3.2 indicates where this investigation's primary and auxiliary data were gathered.

Table 3. 2: Secondary data source

GIS Data Layer	Data Description	Data Source
Vector (polygon)	Woreda Boundary	Ethio-GIS
Vector (line)	River, Contour & Roads	CSA
Vector (point)	Major City	Ethio-GIS
Raster	Elevation & Slope	SSGI
Attribute Table	Rainfall & Tempter	National Meteorological Agency
Attribute Table	Population	CSA

Software’s

The following software programs was utilized to process satellite imagery and assess changes in LULC, NDVI, NDBI and LST (Table 3.3).

Table 3.3: Software’s used for the study

S. No	Software	Function
1	Arc-GIS 10.8	Data presentation, analysis and mapping etc.
2	Edra’s Imagine 2015	Image classification, accuracy assessment etc.
3	Google Earth pro	LULC validation, study area visualization etc.

Methods

The first step in the methodology used in this study to accomplish the research goals was the acquisition of Landsat imagery for the years 1990, 2007, and 2024. These images were sourced from the Earth Explorer website (USGS) and Landsat 8 data was obtained from Libra Development Seed. The selection of these years was based on the availability of the required data. The images acquired or downloaded were taken during the dry season, ensuring cloud-free conditions for accurate analysis. Figure 3.7 illustrates the general methodological flow chart of the study.

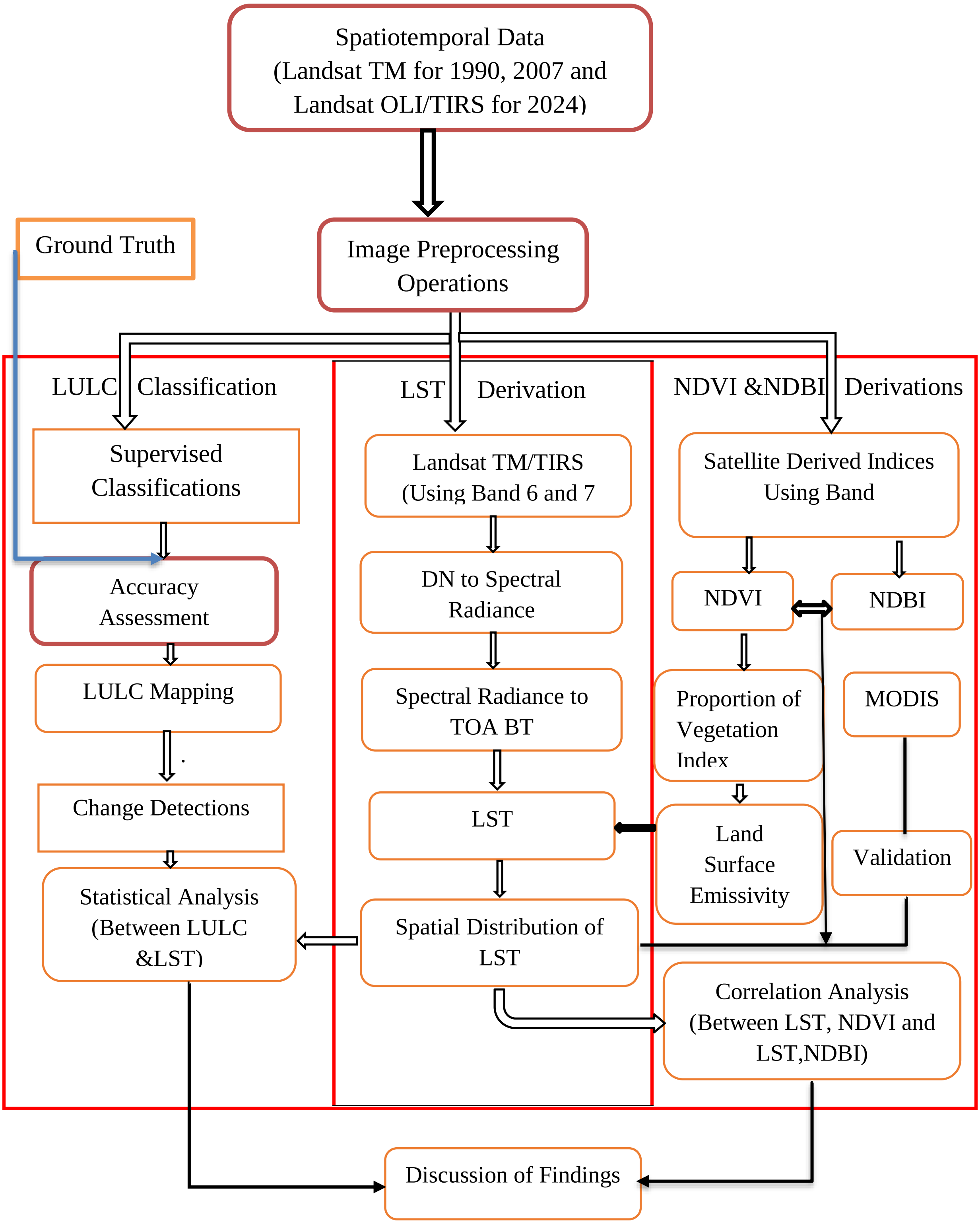

Fig 3.7: Methodological flow chart of the study

3.4 Data Analysis

3.4.1 Digital Image Preprocessing

These methods aim to correct damaged or distorted image data in order to create a more realistic representation of the original scene and improve a picture's readiness for further processing. Typically, this means first processing the raw image data to eliminate noise, then calibrating the data radiometrically and correcting for geometric distortions, and finally using mosaicking or sub setting to expand or contract the extent of an image.

A method to enhance the usability of images for additional analysis and producing a more realistic depiction of the original scene is called digital image processing, or DIP. These procedures aim to improve distorted or subpar image data so that it can be used for a variety of purposes. Digital images, which are numerical representations of two-dimensional scenes made up of pixels, are processed and interpreted by computer software. It is necessary to preprocess raw image data in order to remove noise, calibrate radiometric data, correct geometric distortions, and change the image's extent through sub-setting or mosaicking. In remote sensing, DIP is traditionally used for two primary purposes: preparing image data for computer-assisted interpretation and enhancing the information for human interpretation. The key objective of these operations is to improve the spectral separability of objects within the image, allowing for better identification and classification.

The Landsat 7 ETM+ Scan-Line Corrector (SLC) Error

Data obtained from Landsat 7 ETM+ after May 31, 2003, are referred to as SLC-off data because the Scan Line Corrector (SLC) failed on that date. This failure caused gaps in the scan lines, making the data less suitable for applications requiring continuous data coverage. For a range of uses, such as change detection, environmental monitoring, land cover classification, and land use analysis, SLC-off data can still be helpful with the right geometric and radiometric adjustments.

Modifying the pixel values to ensure accurate reflectance or radiance measurements of the Earth's surface is known as radiometric correction. By removing distortions brought on by platform and sensor features, geometric correction, on the other hand, guarantees that the image is appropriately spatially represented. Despite the gaps caused by the SLC failure, Landsat 7 SLC-off data can still provide valuable insights when analyzed carefully. Users must implement necessary precautions and be mindful of the limitations posed by the data gaps when evaluating and interpreting the imagery.

3.4.2 Image Classification

The categorization process involves assigning each pixel in a digital image to one of many land cover categories, or themes. Thematic maps of the land cover shown in an image and/or summary statistic on the regions covered by each category of land cover can subsequently be created using this classified data. To calculate the LULC of the study area, a maximum likelihood algorithm classification approach under the supervision of GIS and ERDAS envisage was employed. The most often used classification technique for RS data is supervised classification using the maximum likelihood (MLC) algorithm (Foody, 2002).

Classification Accuracy Assessment

Following the land cover categorization process, it is crucial to document the categorical accuracy of classification results. The classification process is not complete until its correctness is assessed, and one of the most widely used methods for assessing classification accuracy is creating an error matrix, also known as a confusion matrix or contingency table, which compares the output of an automated classification method category-by-category with known reference data, or ground truth. The matrix gives an indication of the effectiveness of the categorization procedure by contrasting these two datasets.

In this study, Google Earth and field survey data were used to evaluate the accuracy of the LULC classification. The land cover and use maps for 1990, 2007, and 2024 were compared to determine the final classification accuracy output. A confusion matrix, which incorporates representative points from each land cover category, was employed to evaluate the accuracy of the classification results.

The confusion matrix compares known reference data (ground truth) with the corresponding outcomes of the automated classification, providing insights into how well the classification system has categorized each land cover type. By using representative locations for each land cover class, the matrix allows for a detailed assessment of classification performance.

Documenting the categorical accuracy of the classification results is crucial at the end of the land cover categorization process. Until the correctness of a classification is evaluated, it remains incomplete. One often used technique to demonstrate classification accuracy is the creation of a classification error matrix. Error matrices are used to compare, category by category, the relationship between known reference data (ground truth) and the associated results of an automated classification. Thus, using representative sites from each category of land cover, a confusion matrix was used to evaluate the classification findings' accuracy.

The following equations (1-4) were applied in order to evaluate accuracy (Abir & Saha, 2021).

$$\text{User Accuracy} = \frac{\text{Correctly classified points in each Catagory (diagonal)}}{\text{Total reference points in each catagory (row total)}} * 100 \quad (1)$$

$$\text{Producer Accuracy} = \frac{\text{Correctly classified points in each Catagory (diagonal)}}{\text{Total reference points in each catagory (column total)}} * 100 \quad (2)$$

$$\text{Overall Accuracy} = \frac{\text{Total correctly classified points (diagonal)}}{\text{Total reference points}} * 100 \quad (3)$$

$$\text{Kappa Coefficient} = \frac{\text{Total Sample*Total Correct sample-} \sum \text{(column total*row total)}}{\text{(Total Sample)}^2 - \sum \text{(column total*row total)}} * 100 \quad (4)$$

Table 3.4: Lists the kinds of LULC along with a description of each

LU/LC Class	Description
Farmland	Areas used primarily for agricultural purposes, including both annual and perennial crop cultivation. This class includes a combination of small rural farms and large-scale agricultural fields, which are vital for food production and rural livelihoods.
Bare Land	Non-vegetated areas such as deserts, exposed rocks, beaches, dunes, salt flats, and eroded soil or quarry sites. These areas are characterized by minimal or no vegetation covers and is often associated with degradation or natural landforms.
Water body	comprises both man-made and natural water features, including reservoirs, ponds, rivers, and lakes. In addition to offering recreational and economic benefit, water bodies are essential for sustaining aquatic life and water supplies.

Settlement	Urban areas including residential, commercial, and industrial buildings. This class encompasses infrastructure such as roads, transportation systems, and urban services, supporting human habitation and economic activities.
Vegetation	Areas dominated by plant life, including forests, grasslands, and scrublands. This class is essential for biodiversity, carbon sequestration, and ecological services like soil protection, water regulation, and climate regulation.

3.4.3 Land Use Land Cover Change Detection

Change detection is the process of identifying and analyzing alterations in specific locations over time. Remote sensing techniques are commonly used to assess these changes by comparing multiple images acquired at different time periods. One of the most widely applied methods for change detection is post-classification comparison.

In this study, LULC changes are analyzed using satellite images from 1990, 2007, and 2024. The study requires the integration of technical processes using ArcGIS software to generate LULC change maps. In the first phase, a table that shows the area coverage in square kilometers and the percentage change for each LULC class in 1990, 2007, and 2024 must be created. To quantify these changes, Equation (1) is applied to calculate the percentage change in LULC.

$$\text{Percentage Change} = (\text{observed Change}) / (\text{Total area}) * 100 \qquad (1)$$

3.4.4 Land Surface Temperature Retrieval

LST values for the research period (1990, 2007, and 2024) are generated using the thermal bands of Landsat images (Landsat 5, Landsat 7 ETM+, and Landsat 8). Landsat 5 uses thermal band 6, while Landsat 8 uses thermal band 10. The LST is derived from thermal bands following the next steps.

A. Conversion of DN to Spectral Radiance

Using the image processing program ArcGIS 10.8, the DN of thermal infrared (TIR) bands was converted into spectral radiance using the Radiative Transfer Equation (RTE), which is displayed in Equations (2) and (3). Regarding Landsat TM:

$$L_{\lambda} = \left(\frac{L_{MAX_{\lambda}} - L_{MIN_{\lambda}}}{Q_{CAL_{MAX}} - Q_{CAL_{MIN}}}\right) * \left(Q_{CAL} - Q_{CAL_{MIN}}\right) + L_{MIN_{\lambda}} \quad (2)$$

In this case, Lλ is the spectral radiance value; QCAL is the quantized calibrated pixel's DN value; LMAXλ is the spectral radiance value in ($Wm^{-2}sr^{-1}\mu m^{-1}$) scaled to QCALMAX; LMINλ is the spectral radiance value in ($Wm^{-2}sr^{-1}\mu m^{-1}$) scaled to QCALMIN; QCALMIN and QCALMAX are the minimum and maximum DN values of the quantized calibrated pixels that correspond to LMINλ and LMAXλ, respectively. For OLI/TIRS on Landsat:

$$L_{\lambda} = M_L \times Q_{CAL} + A_L, \quad (3)$$

For example, Lλ is the top of the atmosphere spectral radiance in (Wm−2sr−1μm−1), ML is the rescaling factor for the radiance multiplicative band derived from metadata (i.e., Radiance_Mult_Band 10), QCAL is the DN value of the calibrated and quantized product pixel, and AL is the rescaling factor for the radiance additive band derived from metadata (i.e., Radiance_Add_Band 10).

B) Conversion of spectral radiance to TOA brightness temperature (BT)

The spectral radiance values of the transformed pixels digital numbers were successfully used to recover the top of atmosphere (TOA) brightness temperature (BT), also known as satellite derived temperature and expressed in Kelvin. Equation was used to calculate the brightness (sensor) temperature values under the uniform emissivity assumption (4).

$$BT = \frac{K_2}{\ln\left(\frac{K_1}{L_{\lambda}} + 1\right)} \quad (4)$$

where Lλ is the spectrum radiance at TOA expressed in ($Wm^{-2}sr^{-1}\mu m^{-1}$), BT is the brightness temperature at the top of atmosphere (TOA) given in ◦K, and K1 and K2 are the thermal conversion constants of the obtained metadata.

C) Derivation of land surface temperature from brightness temperature (BT)

Equation (5) is then used in the study to compute the corrected LST (in Kelvin) with the help of the at-satellite brightness temperature (BT).

$$LST(^{\circ}K) = \frac{B_T}{[1 + \lambda\left(\frac{B_T}{E}\right)\ln(\varepsilon)]} \tag{5}$$

In this case, BT is the brightness temperature at-satellite (sensor); λ is the wavelength of radiation emitted (11.5 µm in Band 6 for Landsat 4/5/7 and 10.8 µm in Band 10 for Landsat 8); E is (h × v)/s (1.4388 × 10^{-2}mK); h is Planck's constant (6.626 × 10^{-34}mK); v is the velocity of light (2.998 × 108 m/s); s is the Boltzmann constant (1.38 × 10^{-23} JK); and ε is the land surface emissivity.

Equation (6) was used in the study to determine the land surface's emissivity (ε).

$$\varepsilon) = N (P_v) + n \tag{6}$$

where Pv is the vegetation proportion given in Equation (7), N is 0.004, and n is 0.986.

$$P_v = \left(\frac{NDVI - NDVI_{min}}{NDVI_{max} - NDVI_{min}}\right)^2 \tag{7}$$

Where NDVI is the DN values derived from the NDVI image; the highest and lowest DN values derived from the NDVI image are denoted by NDV_{Imax} and NDV_{Imin}, respectively. Finally, Equation (8) was used to convert the land surface temperature value (in Kelvin) into degrees Celsius (◦C).

$$LST (^{\circ}C) = LST (^{\circ}K) - 273.15 \tag{8}$$

D) Validation of estimated LST

Verification is essential to ensure that the data is suitable for its intended use. To achieve this, a random sample of sites is selected from Google Earth, and zonal statistics from both MODIS daytime and Landsat 8 TIRS LST are used to extract LST values. Ultimately, the average values of each polygon are compared.

E) Normalized Difference Vegetation Index (NDVI) Estimation

One of the most used urban climate indicators in environmental research is the NDVI, an objective index for determining vegetation conditions from remotely sensed data. NDVI is essential for predicting LST since it is directly used to compute land surface emissivity (Guha & Govil, 2020). Positive NDVI values indicate vegetated areas, whereas negative values indicate non-vegetated areas. The NDVI scale runs from -1 to +1. Equation (9), was used to extract the research area's NDVI.

$$NDVI = \frac{NIR\ (Band\ 4,5) - RED\ (Band\ 3,4)}{NIR\ (Band\ 4,5) + RED\ (Band\ 3,4)} \tag{9}$$

Where Landsat 4–5 TM and Landsat 7 ETM+ use NIR (Band 4) and Landsat 8 OLI uses NIR (Band 5). Landsat 4–5 TM is represented by RED (Band 3), while Landsat 8 OLI is represented by RED (Band 4).

F) Normalized Difference Built-Up Index (NDBI) Estimation

The Difference Normalized Another essential urban climate indicator for environmental monitoring is the NDBI. This gives information on the spatial extent of impervious surfaces and built-up regions, making it a useful tool for mapping and assessing land usage.

The mid- and near-infrared bands shown in Equation (10), was used to determine NDBI.

$$\mathrm{NDBI} = \frac{\mathrm{MIR(Band\ 5,6)} - \mathrm{NIR\ (Band\ 4,5)}}{\mathrm{MIR(Band\ 5,6)} + \mathrm{NIR\ (Band\ 4,5)}} \qquad (10)$$

In this study, Landsat 4–5 TM and Landsat 7 ETM+ are represented by the Middle Infrared (MIR) band (Band 5), while Landsat 8 OLI uses MIR (Band 6). For the Near Infrared (NIR) band, Landsat 4–5 TM uses Band 4, whereas Landsat 8 OLI uses Band 5 for NIR.

Statistical Analysis

Statistical analysis is essential for examining the relationship between multiple variables, both independent and dependent. This study analyzes the association between LULC changes and LST using statistical methods. Additionally, linear regression is applied to evaluate the relationship between LST, NDVI, and NDBI.

To achieve this, the pixels in the study area are converted into point data. The parametric values of these points are then extracted using sample points from the derived maps for each study period. The methodological steps followed in this analysis are summarized in the flowchart presented in Figure 3.2.

Model Validation for LST Analysis using Google Earth Pro

The validation of the generated LST maps is conducted using a systematic approach that incorporates Google Earth Pro as a key tool for cross-referencing and verification. The process you're describing is essential for ensuring the accuracy and reliability of the analysis when evaluating the impact of urban expansion on LST in Bishoftu city, Ethiopia.

Google Earth Pro provides high-resolution imagery and historical datasets, facilitating the identification and verification of urban expansion patterns, land use/land cover changes, and their corresponding impact on surface temperature. The validation process includes overlaying LST maps with urban boundary changes derived from temporal satellite images and field surveys. This enables precise spatial alignment and comparison of geospatial outputs with observed urban dynamics.

Additionally, ground-truth temperature data from meteorological stations are utilized to validate LST values. The integration of high-resolution imagery, temporal datasets, and field observations enhances the overall accuracy and reliability of the LST analysis. The combined use of Google Earth Pro and in-situ temperature records ensures that the geospatial methodology provides credible insights into the thermal impact of urban expansion.

CHAPTER FOUR

4. RESULT AND DISCUSSION

The study outcomes were thoroughly examined using a rigorous and systematic approach. The spatial patterns of LST, NDVI, and NDBI were the main focus of this study, which made it possible to fully comprehend both their separate and combined effects. A detailed investigation of the interactions and influences among these factors was conducted, considering the complex relationships that exist among them. The historical trends in LULC were also explored in depth, providing valuable context for the analysis. The analysis involved a comprehensive statistical examination of the relationships among LST, LULC, and spectral indicators, like NDBI and NDVI, which helped identify any correlations or patterns that may exist between these factors. This statistical examination was crucial for providing a more nuanced and accurate understanding of the results.

4.1. LULC Change of Bishoftu city in 1990, 2007 and 2024

The LULC transformations in Bishoftu city between 1990 and 2024 exhibit significant changes driven by urban expansion, agricultural decline, and environmental dynamics. Although the city's total land area remains constant at 542.6512 km², notable alterations have been observed in various LULC classes.

Among the many substantial transformations is the rapid growth of urban regions, which increased from 15.59 km² in 1990 to 69.90 km² in 2024, marking a net increase of 54.31 km² (348.45%). This growth is largely attributed to urbanization, infrastructure development, and population expansion, positioning Bishoftu as a key economic and residential center near Addis Ababa.

In 1990, agricultural land dominated the area, covering 484.17 km². However, by 2024, it decreased to 438.61 km², showing a reduction of 45.56 km², or a 9.41% decline. This loss is mainly due to land conversion for urban settlements, industrial zones, and infrastructure projects, raising concerns about food security and rural livelihoods.

Bare land experienced dynamic fluctuations. It initially expanded from 7.57 km² in 1990 to 13.32 km² in 2007 before drastically decreasing to 0.97 km² in 2024. The initial increase may have been driven by deforestation and land degradation, while the recent decline suggests land reclamation, afforestation, or urban expansion into previously vacant areas.

Vegetation cover exhibited minor changes, increasing from 27.99 km² in 1990 to 33.92 km² in 2007 before decreasing to 26.13 km² in 2024. The net loss of 1.86 km² suggests that afforestation efforts were insufficient to counteract deforestation and urban expansion. This reduction raises concerns about biodiversity loss, soil degradation, and the city's resilience to climate change.

Water bodies underwent fluctuations, decreasing from 7.32 km² in 1990 to 5.42 km² in 2007 before partially recovering to 7.03 km² in 2024. The initial decline may be attributed to increased water consumption, sedimentation, and pollution, while the recent increase likely results from conservation efforts and improved water management.

The findings highlight a clear trend towards urbanization, emphasizing the need for sustainable land-use planning. The loss of agricultural land and vegetation underscores the importance of policies that integrate urban expansion with environmental conservation, while the stability of water resources demands continued monitoring and protection.

Table 4.1 LULC area and change of the study area in 1990, 2007, and 2024

LU/LC Classes	1990 Area (km²)	2007 Area (km²)	2024 Area (km²)	1990–2007 Change (km²)	2007–2024 Change (km²)	1990–2024 Change (km²)
Agriculture	484.13	451.39	438.61	-32.78	-12.78	-45.56
Bare Land	7.57	13.31	0.96	5.75	-12.35	-6.61
Built-up	15.58	38.59	69.90	23.01	31.31	54.31
Vegetation	27.99	33.92	26.13	5.93	-7.79	-1.86
Water	7.3205	5.4215	7.033	-1.9	1.61	-0.29

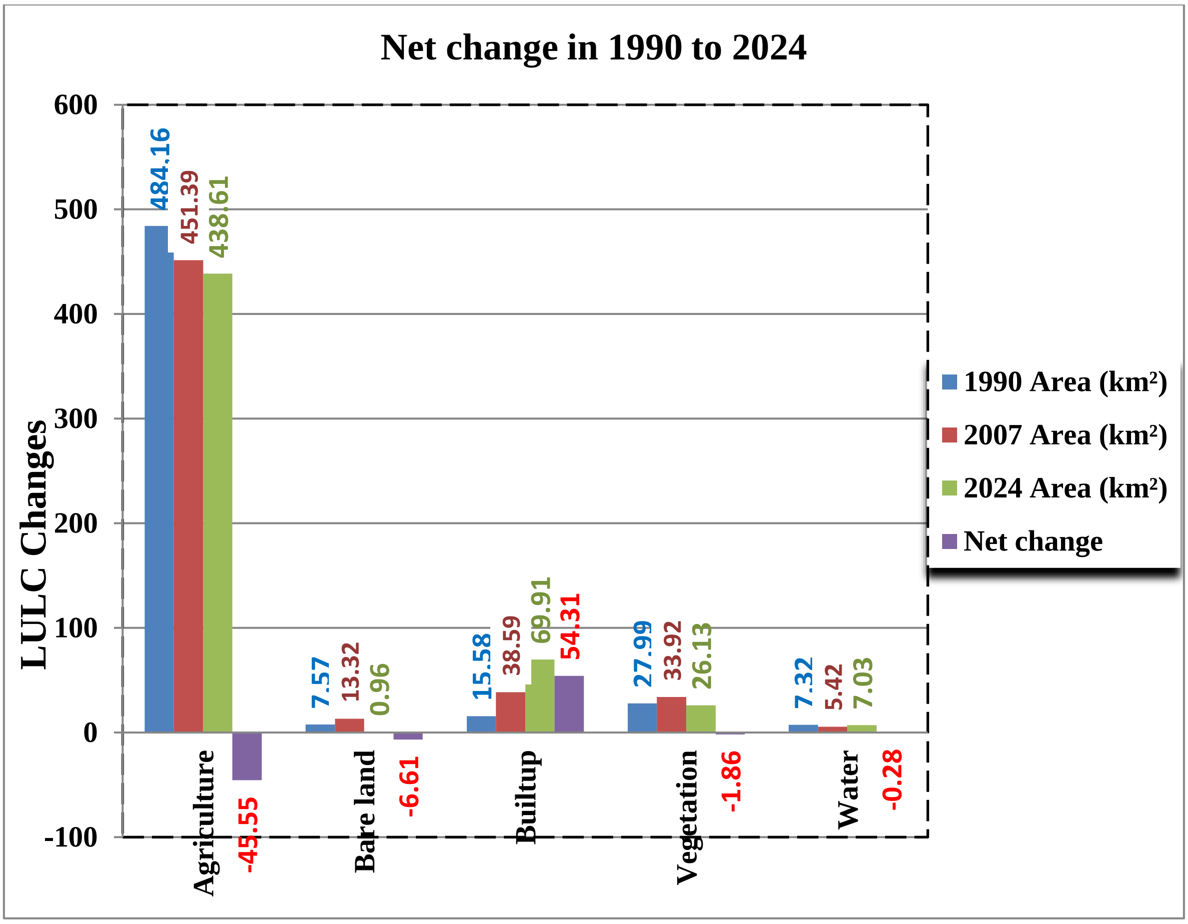

Fig 4.1: LULC area and changes of the study

The LULC changes in Bishoftu city between 1990 and 2024 are described by a dynamic transformation driven by rapid urbanization, declining agricultural land, fluctuating vegetation cover, and minor changes in water bodies. The primary change is the growth of built-up regions, which is mostly attributable to infrastructural development and population expansion. This urban growth presents opportunities for economic development, but it also poses challenges related to land use, environmental degradation, and resource management. Policymakers and urban planners must adopt comprehensive strategies that balance economic expansion with environmental conservation to ensure sustainable urban development. Implementing sustainable land-use planning, promoting green infrastructure, and strengthening resource management policies is crucial in maintaining ecological balance while accommodating future urban growth in Bishoftu.

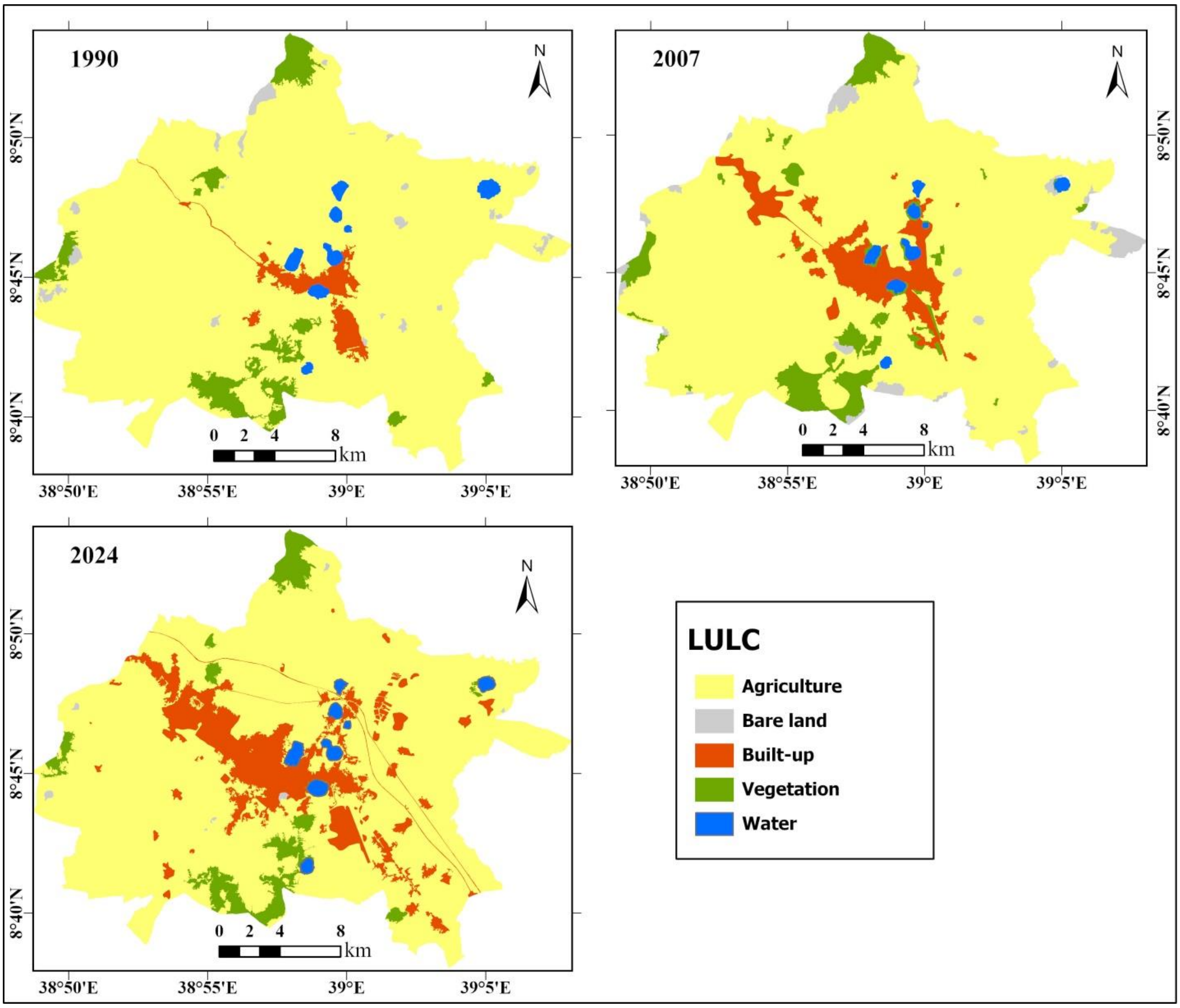

Fig 4.2: Maps showing the LULC of study area

4.1.1 Geographical extent and spatial distribution of LULC

The spatial distribution of LULC changes in Bishoftu city between 1990 and 2024 reveals significant transformations across five major LULC classes. Over the 34-year study period, agricultural land, which was the predominant land use in 1990, covered 89.27% of the total area. However, this decreased to 83.21% in 2007 and further declined to 80.85% in 2024, marking a total reduction of 8.42%. Urbanization and land conversion for infrastructural development are the main causes of this reduction.

Bare land exhibited fluctuations, increasing from 1.40% in 1990 to 2.45% in 2007 before dropping sharply to 0.18% in 2024. The net reduction of 1.22% suggests successful land reclamation efforts and urban encroachment into previously barren areas. In contrast, built-up land showed the most significant increase, rising from 2.87% in 1990 to 7.11% in 2007 and further to 12.89% in 2024. This marks a 10.02% rise, emphasizing the rapid pace of urbanization and infrastructure development within the city.

Vegetation cover displayed minor variations, constituting 5.16% of the total area in 1990, increasing to 6.25% in 2007, and then declining to 4.82% in 2024. The influence of agricultural and urban growth on vegetative areas, which results in deforestation, is indicated by the net loss of 0.34%. Similarly, water bodies, which accounted for 1.35% of the total area in 1990, decreased to 1.00% in 2007 before slightly recovering to 1.30% in 2024. This minor decline of 0.05% highlights the relative stability of water resources despite urbanization pressures.

Rapid urban expansion is reflected in the 5,671.09 hectares of agricultural land that were transformed into built-up areas, according to additional analysis of land conversion patterns. Additionally, afforestation initiatives or natural regeneration processes were shown by the 656.16 hectares of agricultural land that turned into vegetation. A smaller area-76.79 hectare-was transformed into bodies of water, most likely due to the growth of wetland. Additionally, bare land was converted; 100.68 hectares were turned into built-up areas, which supported urban growth, while 606.97 hectares were reclaimed for agricultural use, indicating better land management methods. Significantly, 104.02 hectares of water bodies were turned into farmland, most likely as a result of increased irrigation.

These transformations underscore a strong shift towards urbanization, with built-up areas expanding significantly at the expense of agricultural and vegetative lands. Urbanization promotes economic progress, but it also brings up issues with resource management, environmental sustainability, and food security. Policymakers must adopt comprehensive land-use strategies, including zoning regulations, the promotion of green infrastructure, and sustainable water resource management, to ensure a balanced and resilient urban future for Bishoftu.

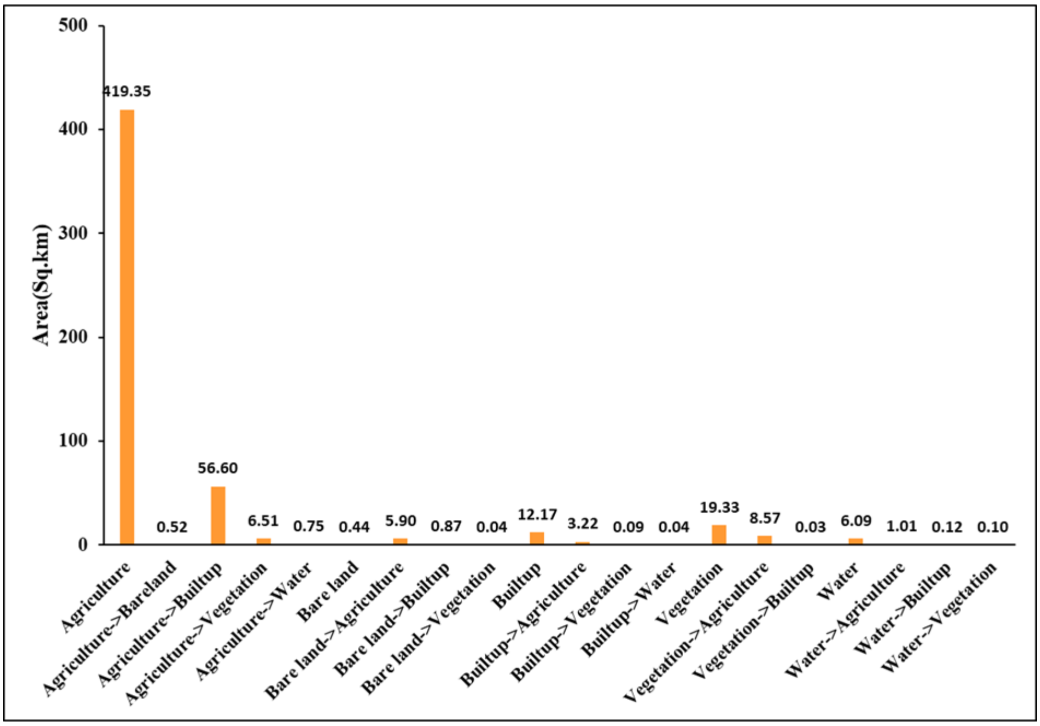

Fig 4.3: LULC Change detection analysis of study area from 1990 to 2024

4.1.2 Accuracy assessment

Strong performance across all classes is indicated by the classification accuracy assessment for the Bishoftu city LULC maps for the years 1990, 2007, and 2024. In 1990, the producer's accuracy (PA) for agriculture was 95.1%, and the user's accuracy (UA) was 96.3%. For bare land, both PA and UA were recorded at 90.0%, while built-up areas had a PA of 93.5% and a UA of 96.7%. Vegetation had a PA of 91.9% and a UA of 85.0%, and water bodies recorded 90.0% for both PA and UA. The 1990 classification had a 91.02% Kappa coefficient and an overall accuracy of 93.5%.

In 2007, agriculture had a PA of 94.9% and a UA of 93.8%, while bare land showed a PA of 81.8% and a UA of 90.0%. Built-up areas had a PA of 92.1% and a UA of 96.7%. Vegetation maintained a PA of 91.9% and a UA of 85.0%, while water remained consistent with 90.0% for both PA and UA. The overall accuracy in 2007 was slightly lower at 92.5%, with a corresponding Kappa coefficient of 89.12%.

By 2024, the accuracy values improved slightly. Agriculture achieved a PA of 96.3% and a UA of 97.5%. Bare land retained a PA and UA of 90.0%. Built-up areas had a PA of 95.1% and a UA of 96.7%. Vegetation showed a PA of 92.1% and a UA of 87.5%. Water bodies continued to maintain a PA and UA of 90.0%. With a Kappa coefficient of 92.04% and an overall classification accuracy of 94.5%, the classified map and the reference data showed very high agreement.

Table 4.2: Accuracy Assessment Results of Classification for 1990, 2007, and 2024

LULC Class	1990 PA (%)	1990 UA (%)	2007 PA (%)	2007 UA (%)	2024 PA (%)	2024 UA (%)
Agriculture	95.1	96.3	94.9	93.8	96.3	97.5
Bare land	90	90	81.8	90	90	90
Built-up	93.5	96.7	92.1	96.7	95.1	96.7
Vegetation	91.9	85	91.9	85	92.1	87.5
Water	90	90	90	90	90	90
Overall Accuracy	93.5		92.5		94.5	
Kappa Coefficient	91.02		89.12		92.04	

4.1.3 Settlement expansion during 1990–2024

Using satellite imagery from 1990, 2007, and 2024, an overlay analysis of Bishoftu city's settlement growth shows a notable rise in built-up regions, underscoring the city's fast urbanization over the previous three decades. The built-up area in 1990 covered 2.87% (15.59 km²) of the total land area, expanding to 7.11% (38.59 km²) in 2007 and further growing to 12.89% (69.90 km²) in 2024. This indicates significant land conversion for residential, commercial, and industrial uses, as evidenced by the 348.45% increase in urban settlements. The Urban Heat Island (UHI) effect, in which temperatures in populated places are higher than in nearby rural areas, has been exacerbated by Bishoftu's urban growth. The UHI effect occurs due to factors such as increased impervious surfaces (roads, concrete, and rooftops), reduced vegetation, and heat absorption by buildings and asphalt. The reflection of sheet metal, dark-colored rooftops, and asphalt roads further intensifies heat accumulation, making urban areas significantly warmer than adjacent non-urban regions. The rising surface temperatures brought on by Bishoftu's ongoing urbanization may have negative effects on the local climate, increase the energy required for cooling, and cause more heat stress for locals.

To mitigate the UHI effect, urban planning strategies should incorporate cool and reflective materials for pavement and rooftops, increase vegetation through tree planting and green spaces, and promote compact growth to reduce unnecessary land consumption. Implementing green roofs, permeable pavements, and urban parks can help absorb heat, improve air quality, and enhance urban resilience to climate change. Additionally, proper zoning regulations and urban airflow management can reduce heat buildup in densely populated areas. Fig. 4.4 shows the settlement area's expansion towards further LULC classes.

In Bishoftu, the overlay analysis of settlement growth emphasizes the necessity of sustainable urban development plans. If the city's fast expansion is not controlled, it could result in more environmental problems, such as warmer surface temperatures, worse air quality, and a further loss of green areas. Bishoftu may strike a balance between environmental sustainability and development by incorporating climate-responsive urban planning techniques, guaranteeing a robust and habitable urban environment for coming generations.

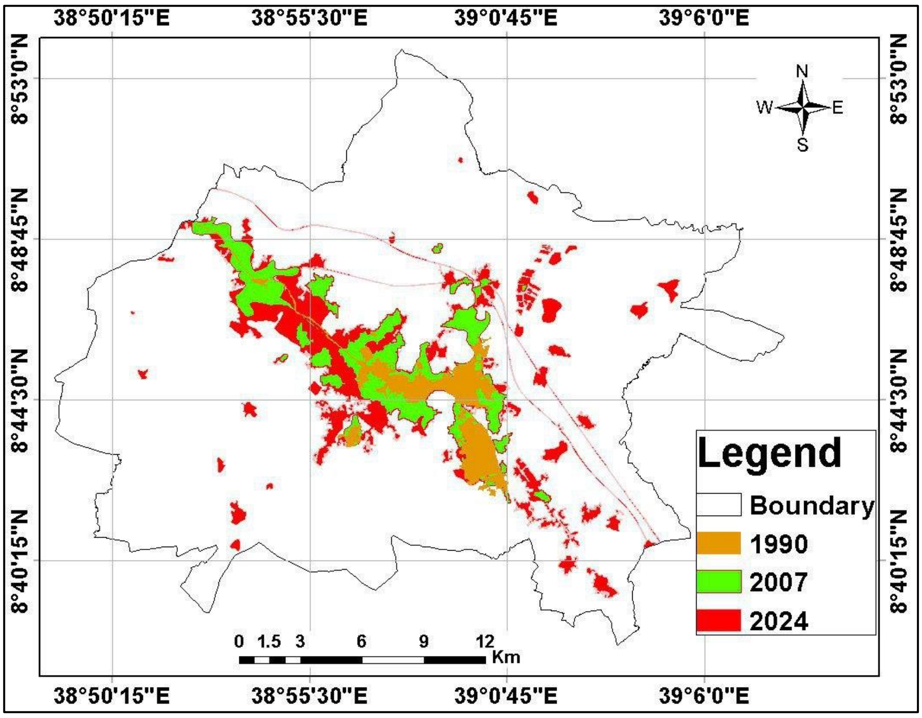

Fig 4.4: The pattern of the settlement area's growth from 1990 to 2024

4.2 Normalized Difference Vegetation Index Analysis in Bishoftu city (1990–2024)

4.2.1 Trends in Vegetation Cover Changes

The NDVI analysis for Bishoftu city between 1990 and 2024 shows a persistent and alarming decline in vegetation cover. The detrimental consequences of urbanization, changes in land use, and environmental degradation are mostly to blame for this loss. The density and condition of the vegetation are accurately represented by the NDVI values, which range from -1 to +1. While lower values suggest bare soil, built-up regions, or damaged vegetation, higher values show dense, thriving vegetation.

The computed NDVI values for the three study years (1990, 2007, and 2024) demonstrate a significant and ongoing loss of vegetation over time. This loss emphasizes how urgently conservation actions are needed. Table 4.3 presents the minimum, maximum, mean NDVI, and standard deviation values, which illustrate the continued decline in green cover over time. This further emphasizes the severity of the issue.

Table 4.3 NDVI Values for Bishoftu City (1990–2024)

Year	Minimum NDVI	Maximum NDVI	Mean NDVI	Standard Deviation (SD)
1990	-0.421	0.607	0.093	0.2968
2007	-0.109	0.43	0.1605	0.1556
2024	-0.184	0.418	0.117	0.1738

In 1990, NDVI values ranged from -0.421 to 0.607, reflecting the presence of substantial green spaces, including forests, grasslands, and agricultural lands. This period represented a time when Bishoftu maintained a relatively healthy natural ecosystem, with a moderate level of urbanization. But by 2007, NDVI readings had dropped to a range of -0.109 to 0.430, showing the loss of vegetation brought on by increased agricultural activity and land conversion for urban growth. The most significant reduction was observed in 2024, where NDVI values dropped to -0.184 to 0.418, indicating further deforestation, urban sprawl, and significant land-use changes.

4.2.2 Spatial Distribution of Vegetation Cover

The spatial distribution of vegetation across Bishoftu has also changed over time, with notable shifts in vegetation-rich areas and non-vegetated zones. The northern and eastern parts of Bishoftu continuously showed higher NDVI values during the study period, showing the existence of green open spaces, forests, and agricultural lands. These areas have historically supported dense vegetation due to favorable land-use policies and lower population density.

On the other hand, non-vegetated areas such as built-up and bare land have grown considerably over time, especially in the city's center and south. The most affected areas correspond to locations where rapid infrastructure development, industrial growth, and population expansion have occurred.

The presence of major water bodies in Bishoftu has contributed to local vegetation stability, as moisture availability supports plant growth. However, fluctuations in water levels and increased human activities around lakes and wetlands have led to partial vegetation loss near these water bodies. By 2024, the impact of urban expansion became more pronounced, with a notable reduction in green cover as settlement areas expanded further, replacing previous vegetative zones.

4.2.3 Urbanization's Impact on the Loss of Vegetation

The declining NDVI values in Bishoftu are strongly correlated with urban expansion, agricultural intensification, and unsustainable land management practices. The city's climate has changed and environmental stresses have increased as a result of the substantial loss of green cover caused by the conversion of agricultural and forestry regions into built-up areas. When plants are replaced with heat-absorbing materials like concrete, asphalt, and metal structures, urbanized areas experience higher surface temperatures. This issue contributes to poor air quality, decreased urban livability, increased energy use, and worsened urban warming. Additionally, the reduction of vegetation cover has further weakened ecosystem services, including:

Decreased carbon sequestration raises carbon dioxide levels in the atmosphere, hastening climate change and its effects. Increased land degradation and soil erosion due to the loss of natural plants that once stabilized the soil. Because fewer wildlife habitats result from the loss of green spaces, biodiversity declines and the ecological balance is upset. Without intervention, continued vegetation loss was result in further environmental degradation, making Bishoftu more vulnerable to climate-related challenges such as heat waves, flash floods, and declining water quality.

4.2.4 Urban Planning Strategies for Vegetation Conservation

Sustainable urban design techniques must be used to strike a balance between ecological preservation and urban growth in order to lessen the detrimental effects of vegetation loss. Several key measures can be adopted to protect and restore vegetation cover in Bishoftu:

a) Afforestation and Reforestation Programs

Large-scale tree planting initiatives should be prioritized to restore degraded lands and enhance urban greenery.

To increase urban biodiversity, native tree species ought to be planted in commercial, industrial, and residential areas.

b) Integration of Green Infrastructure

Urban parks, tree-lined streets, and green belts should be incorporated into new and existing urban developments.

The promotion of rooftop gardens, vertical green walls, and permeable pavements can help enhance vegetation cover in high-density urban areas.

c) Strengthening Land-Use Policies

Land-use regulations should ensure the protection of existing green spaces and limit excessive land conversion for non-vegetative purposes.

Development guidelines should include mandatory green spaces within new residential and commercial areas.

d) Urban Agriculture and Community Greening Programs

Encouraging urban farming and home gardening can help increase greenery within residential and commercial zones.

Community-led tree planting campaigns can raise awareness and encourage public participation in greening efforts.

e) Climate-Resilient Building Materials and Urban Design

Reflective and heat-resistant building materials should be promoted to reduce heat absorption and minimize urban warming.

The design of climate-resilient buildings should integrate natural ventilation, shading, and energy-efficient cooling solutions to counteract heat accumulation.

In order to preserve ecological balance, urban resilience, and environmental sustainability, sustainable land management techniques are desperately needed, as seen by the diminishing NDVI trends seen in Bishoftu. Early greening initiatives can be used to regulate urban growth in a way that promotes environmental preservation and economic growth. This was ensuring that Bishoftu remains a livable, sustainable, and climate-resilient city for future generations.

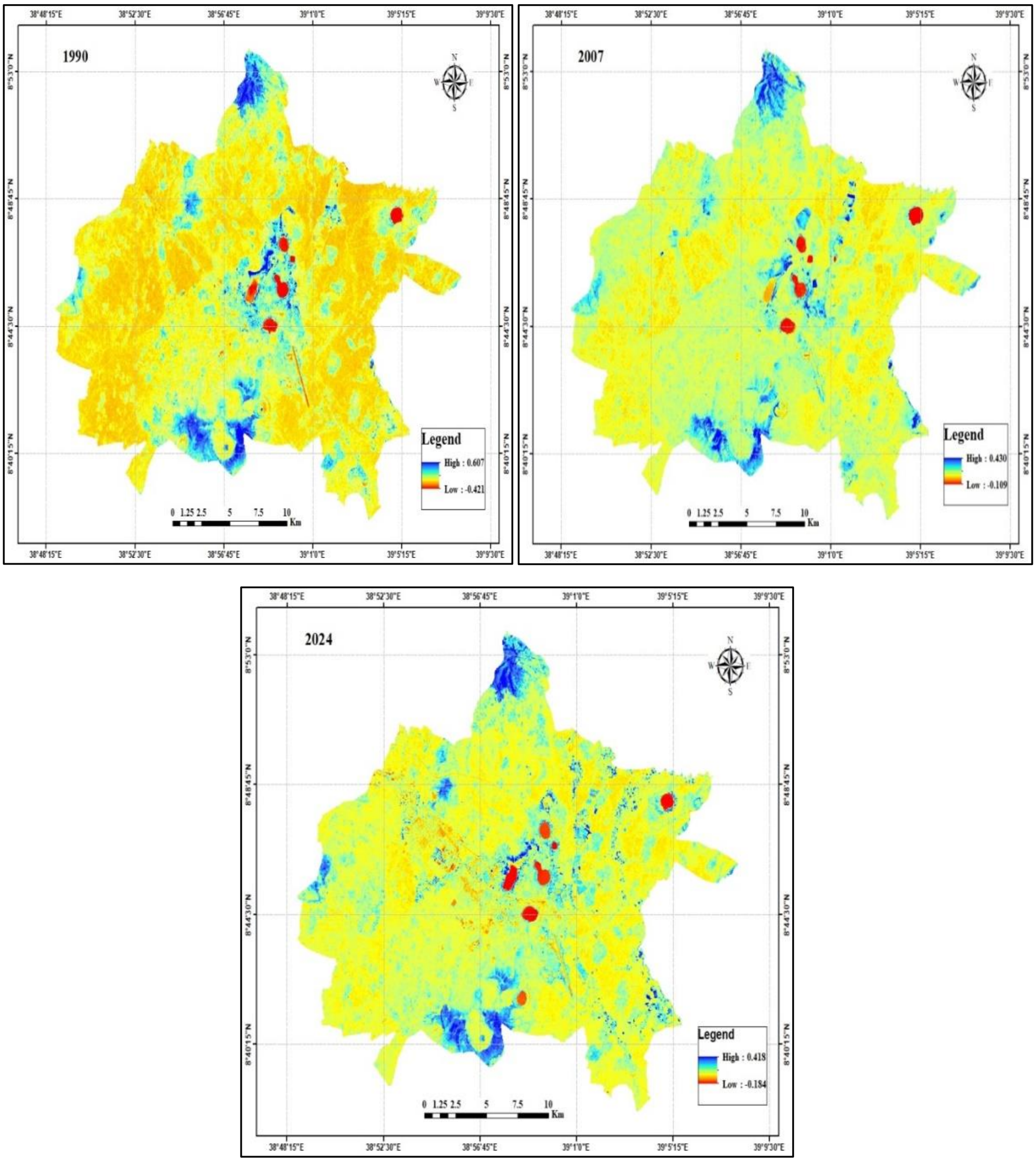

Fig 4.5: Study area NDVI maps (1990, 2007, and 2024)

Table 4.4. Changes in Mean NDVI Values for Different LULC Classes in Bishoftu city (1990–2024)

LU/LC Classes	1990 Mean NDVI	2007 Mean NDVI	2024 Mean NDVI	1990–2007 Change in NDVI	2007–2024 Change in NDVI	1990–2024 Change in NDVI
Agriculture	0.514	0.27	0.301	-0.24	0.031	-0.213
Bare Land	0.421	0.109	0.18	-0.312	0.075	-0.237
Built-up	0.607	0.43	0.43	-0.17	-0.012	-0.189
Vegetation	0.607	0.43	0.301	-0.17	-0.129	-0.306
Water	0.421	0.43	0.418	0.009	-0.012	-0.003

4.3 Relationship between LULC and NDVI

The relationship between LULC and the NDVI offers important information on the density and health of plants over time across various land cover types. NDVI, derived from the near-infrared (NIR) and red spectral bands of satellite imagery, is an essential indicator of vegetation vigor and is widely used to assess land cover changes and their environmental impacts (Pettorelli et al., 2005).

Spatial and Temporal Trends in NDVI

There are notable differences in the NDVI values between the various LULC classes during the research periods of 1990, 2007, and 2024 (Table 4.3). The results show that whereas built-up and bare terrain areas have lower NDVI values, vegetation-dominated areas typically have higher NDVI values. Over the three decades, substantial changes in NDVI values have been observed, reflecting shifts in land cover and land use patterns.

NDVI Trends in Vegetation-Dominated Areas

According to earlier research that emphasizes the close relationship between NDVI and vegetative biomass, the regions with the highest NDVI values were those that were primarily covered by forests and shrub land (Xie et al., 2022). The NDVI values of these ecosystems were steady in 1990, but they gradually declined in 2007 and 2024, showing that anthropogenic activities like urbanization and deforestation were causing vegetation loss.

NDVI Variability in Other LULC Classes

Throughout all research periods, built-up areas—which are defined by the development of infrastructure—showed consistently low NDVI values. The built-up regions' NDVI decreased from 0.607 to 0.418 between 1990 and 2024, indicating a rise in impervious surfaces and a commensurate decrease in plant cover. In a similar vein, barren land had the lowest NDVI values, declining sharply from 1990 to 2007 (-0.312) before slightly increasing from 2007 to 2024 (+0.075). This raises the possibility of seasonal vegetation regeneration or possible land reclamation initiatives in some places. Agricultural lands showed moderate NDVI values, reflecting variations in cropping intensity and land management practices. The NDVI of agricultural areas declined sharply from 1990 to 2007 (-0.2445), likely due to land degradation, increased tillage, and conversion to built-up areas. From 2007 to 2024 (+0.0315), there was a minor rebound, nevertheless, which might have been brought about by better farming methods or afforestation initiatives.

Implications of NDVI Changes

The study area's overall vegetation cover is declining, according to the reported NDVI trends, mostly as a result of land-use changes and urbanization. The reduction in NDVI values aligns with findings from similar studies that associate increased urbanization with declining vegetation indices (Zhang et al., 2018). Important environmental effects of this reduction include decreased biodiversity, elevated land surface temperatures, and decreased carbon sequestration.

The need for sustainable land-use plans to reduce vegetation loss is further shown by the regional study of NDVI trends. Integrating green infrastructure and afforestation initiatives can help stabilize NDVI values and support ecological resilience in urbanizing landscapes (Huang et al., 2020).

The NDVI maps for 1990, 2007, and 2024 (Figure 4.5) provide a visual representation of the temporal changes in vegetation distribution, illustrating the effects of LULC transformations over time. These results underscore the critical role of remote sensing techniques in monitoring land cover dynamics and informing sustainable land management strategies.

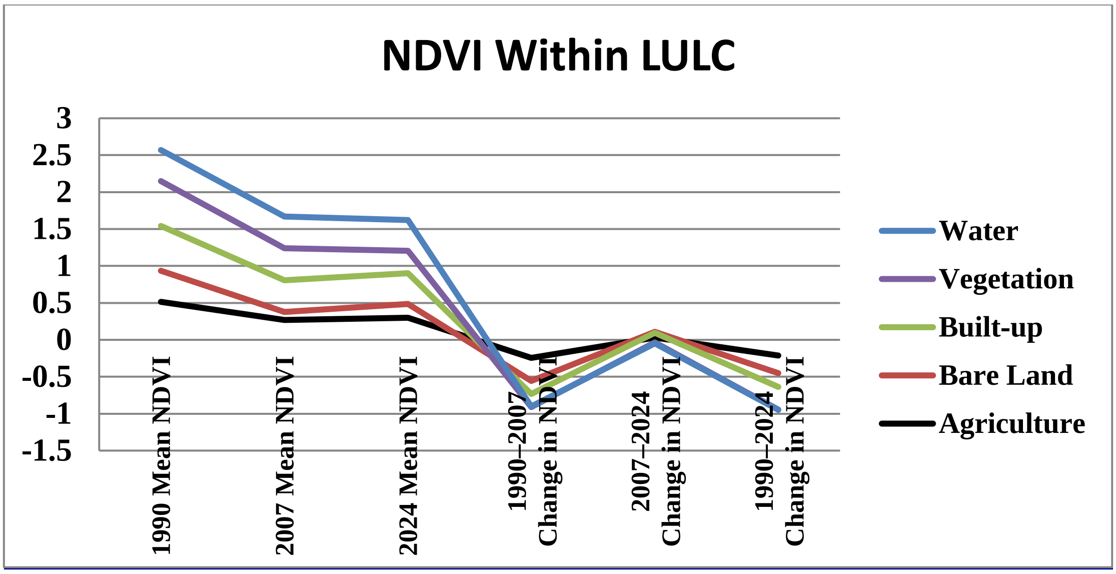

Fig 4.6: Relationships between LULC and NDVI in Bishoftu city (1990–2024)

4.4 Normalized Difference Built up Index (NDBI) Analysis in Bishoftu city (1990–2024)

The analysis of the NDBI for Bishoftu city between 1990 and 2024 reveals significant trends in the expansion of built-up areas over the three decades. NDBI, derived from remote sensing data, is widely used to assess urban expansion and changes in built-up areas (Zha et al., 2003).

In 1990, the NDBI values showed a relatively low level of urbanization, with a minimum of -0.353, a maximum of 0.034, and a mean of -0.281. This indicated that non-built-up areas, such as vegetation, bare land, and water bodies, dominated the landscape, with very limited built-up areas. However, by 2007, the NDBI values began to show a slight shift towards more urbanization, with a minimum value of -0.360 and a mean of -0.317, indicating a gradual increase in built-up areas. The maximum NDBI value of 0.033 in 2007 highlighted the expansion of urban areas, although these changes were still relatively modest compared to other land covers like vegetation and bare land.

By 2024, the NDBI values indicated a marked increase in built-up areas, with a minimum of -0.562, a maximum of 0.258, and a mean of -0.594. This suggests a substantial expansion of the built-up areas, particularly in the urban core and surrounding regions, which is reflected in the wider range of NDBI values between -0.562 and 0.258. The shift towards more positive NDBI values shows that the contrast between built-up and non-built-up areas has become more pronounced. This indicates that urbanization in Bishoftu City has significantly accelerated, with a noticeable reduction in non-built-up areas, which could be attributed to factors such as population growth, infrastructure development, and economic expansion.

The trend of increasing built-up areas over the three decades highlights the rapid urbanization of Bishoftu city. The expansion of urban areas, especially between 2007 and 2024, is likely driven by increased demand for housing, commercial development, and improved infrastructure. However, this growth also suggests potential environmental concerns, such as the reduction of green spaces, the formation of urban heat islands, and changes to local hydrological cycles. The decrease in natural land covers may lead to challenges in managing biodiversity, water resources, and overall environmental sustainability in the face of ongoing urban expansion.

Table 4.5: NDBI Values for Bishoftu City (1990–2024)

Year	Minimum NDBI	Maximum NDBI	Mean NDBI	NDBI Range (Min-Max)
1990	-0.353	0.034	-0.281	-0.353 to 0.034
2007	-0.36	0.033	-0.317	-0.360 to 0.033
2024	-0.562	0.258	-0.594	-0.562 to 0.258

The findings align with previous research indicating that rapid urbanization significantly alters land cover composition, contributing to changes in local climate and ecological balance (Xu, 2008). Future studies should focus on sustainable urban planning strategies to mitigate the environmental impacts of rapid urban expansion in Bishoftu city.

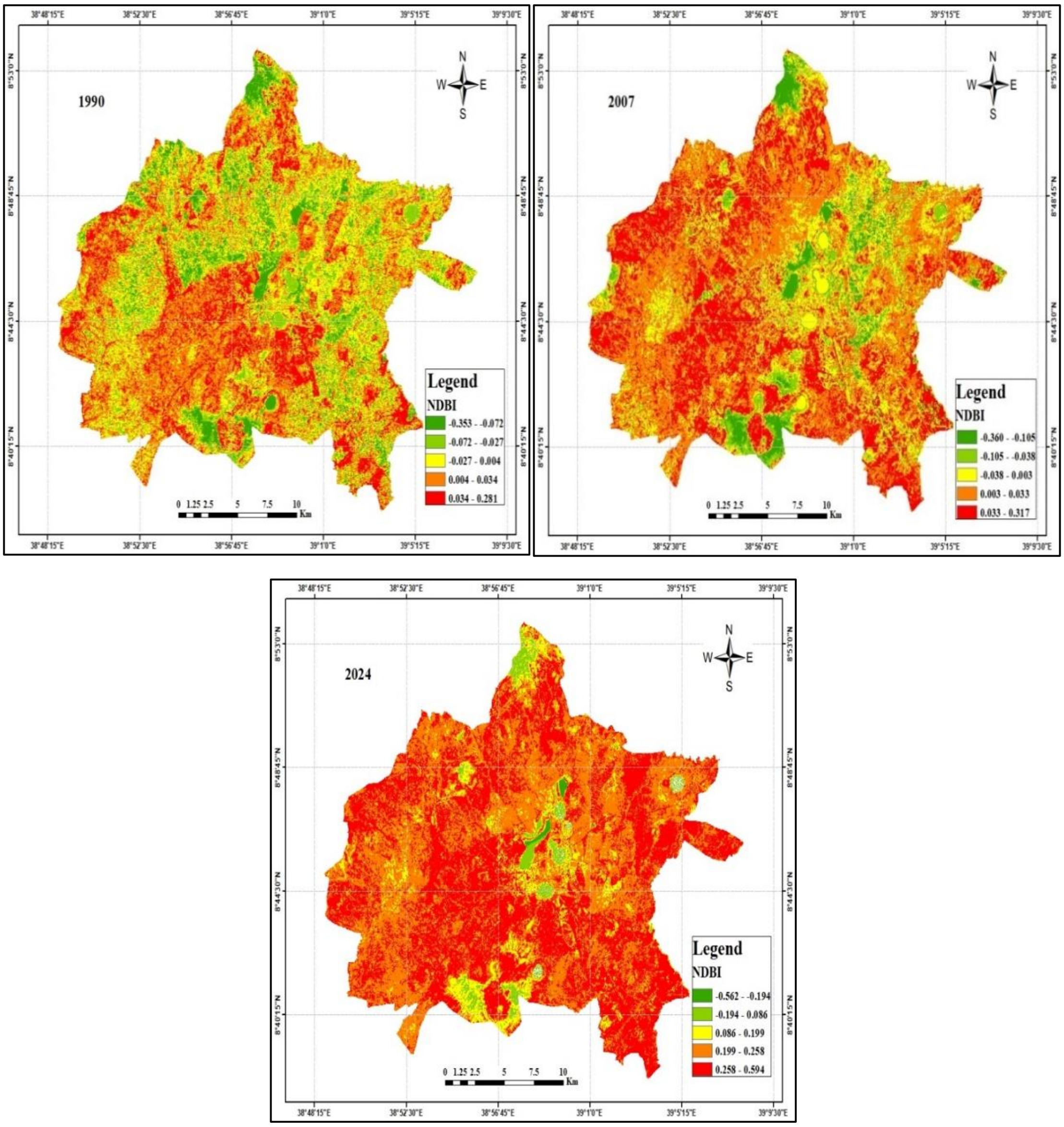

Fig.4.7: NDBI Maps of Bishoftu city (1990, 2007, and 2024)

4.4.1 LULC and the NDBI Relationship in Bishoftu City (1990–2024)

The substantial influence of urbanization on the environment is highlighted by the relationship between LULC changes and NDBI in Bishoftu city between 1990 and 2024. Between 1990 and 2024, built-up areas expanded dramatically from 15.59 km² to 69.90 km², a growth of 348.45%, at the expense of agricultural land, which decreased by 45.56 km² (9.41%). Agricultural land and natural vegetation are being converted into constructed environments as a result of this urban expansion, which is primarily driven by population growth and rising infrastructural demand. As a result, bare land initially increased from 7.57 km² in 1990 to 13.32 km² in 2007 but then sharply declined to 0.97 km² by 2024. Vegetation cover fluctuated during this period, first increasing from 27.99 km² to 33.92 km² in 2007, but then fell back to 26.13 km² by 2024, further emphasizing the loss of green spaces due to urban sprawl.

The NDBI values reveal a clear correlation with the growth of built-up areas and urbanization trends. In 1990, NDBI values were low, with a minimum of -0.353 and a maximum of 0.034, indicating limited urbanization. However, by 2007, NDBI values showed a shift toward urbanization, and by 2024, the values had significantly increased, reflecting a more pronounced urban core with a minimum of -0.562 and a maximum of 0.258. These changes highlight the growing dominance of impervious surfaces and the transformation of natural land covers into urban areas. The increasing contrast between built-up and non-built-up regions, as seen in both LULC and NDBI trends, signals the need for sustainable urban planning to mitigate potential environmental challenges such as biodiversity loss, soil degradation, and the exacerbation of urban heat island effects.

Table 4.6 LULC and NDBI Changes in Bishoftu city (1990–2024)

Year	Built-up Area (km²)	Agricultural Land (km²)	Bare Land (km²)	Vegetation (km²)	Water Bodies (km²)	Min NDBI	Max NDBI	Mean NDBI
1990	15.59	486.04	7.57	27.99	7.32	-0.353	0.034	-0.281
2007	38.59	440.48	13.32	33.92	5.42	-0.36	0.033	-0.317
2024	69.9	440.48	0.97	26.13	7.03	-0.562	0.258	-0.594

4.5 Spatiotemporal Distribution of Land Surface Temperature

Analyzing the spatial distribution of LST is crucial for understanding various environmental factors such as evapotranspiration, temperature variations, and urban climate dynamics (Govind and Ramesh, 2019). Changes in LST can indicate shifts in land use, urban expansion, and climate conditions, making it an essential parameter for environmental assessments.

In this study, LST was retrieved using thermal bands from different Landsat sensors. For the years 1990 and 2007, Landsat 5 and 7 (Thermal Band 6) were used to estimate LST. Meanwhile, for the year 2024, Landsat 8 (TIRS Bands 10 and 11) was utilized. The LST values were extracted and mapped for Bishoftu city using ArcGIS software, allowing for a comparative analysis of spatiotemporal variations over the study period.

The results show that the minimum and maximum LST values varied across the years. In 1990, LST ranged between 8.74°C and 38.2°C. By 2007, the temperature range had slightly increased to 17.17°C - 41.22°C, while in 2024, it further rose to 30.09°C – 48.43°C. These temperature shifts indicate a progressive warming trend in Bishoftu city. In all LST maps, bright reddish tones represent areas with higher surface temperatures, while bluish tones indicate cooler regions.

A detailed comparison of LST values reveals a significant increase over time. Between 1990 and 2007, the maximum LST increased from 38.2°C to 41.22°C, while the minimum LST rose from 8.74°C to 17.17°C. The increase in LST during this period suggests that urbanization and land cover changes contributed to rising surface temperatures.

Between 1990 and 2024, a more substantial warming trend was observed. The mean LST increased from 23.47°C to 39.26°C, indicating a notable rise in temperature over the 34-year period. Both the maximum and minimum LST values also showed significant increases, further confirming the warming trend (Figure 4.8 and Table 4.6). These changes highlight the impact of urbanization, deforestation, and land cover modifications on surface temperature dynamics.

Table 4.6 Mean Temperature of 1990, 2007 and 2024

Year	Minimum LST (°C)	Maximum LST (°C)	Mean LST (°C)	Standard Deviation (°C)
1990	8.74	38.2	23.47	7.87
2007	17.17	41.22	29.2	6.01
2024	30.09	48.43	39.26	4.09

The increasing LST values observed in Bishoftu emphasize the need for sustainable urban planning and climate adaptation strategies. Implementing measures such as green infrastructure, afforestation, and improved land management practices could help mitigate the effects of rising surface temperatures and enhance urban resilience.

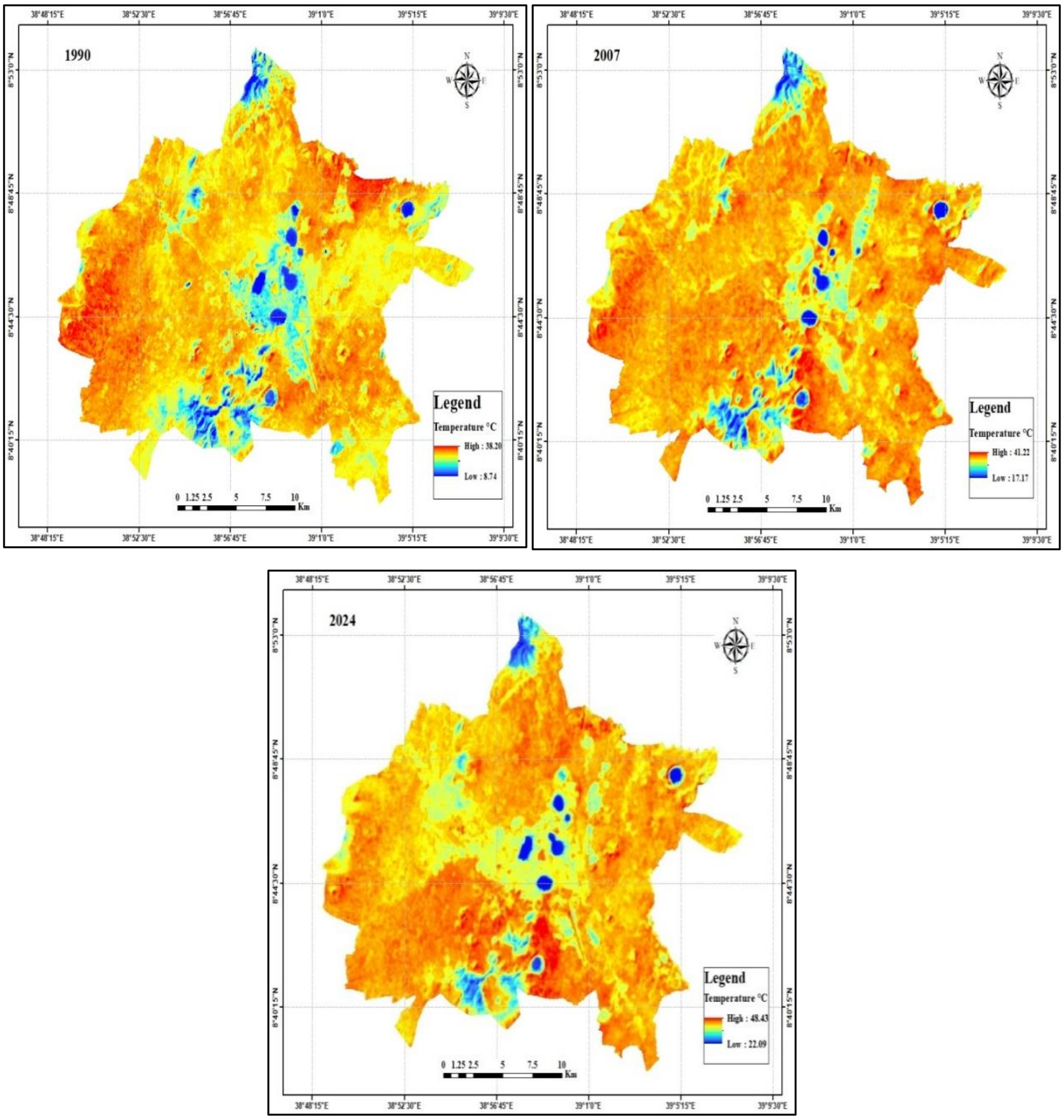

Fig 4.8: Spatial Distribution of LST in Bishoftu (1990–2024)

4.5.1 Changes in LULC and their effects on LST

The analysis of LULC changes and their impact on LST reveals significant warming trends across different land cover types in Bishoftu. The temperature of agricultural areas increased by 1.12°C from 1990 to 2007, followed by a more pronounced rise of 9.67°C from 2007 to 2024. This increase suggests a shift in land management practices, such as intensified agricultural activities and reduced vegetation cover, which contribute to rising surface temperatures.

Similarly, bare land experienced a steady temperature increase of 1.59°C between 1990 and 2007, with a larger rise of 9.13°C from 2007 to 2024. The substantial increase in bare land temperature is likely attributed to soil exposure, reduced vegetation cover, and increased solar radiation absorption. As land degradation progresses, the ability of the land surface to retain moisture decreases, leading to higher surface temperatures.

Built-up areas exhibited the most notable temperature rise among all LULC classes. The temperature increased by 4.01°C from 1990 to 2007, followed by a sharp rise of 9.75°C from 2007 to 2024. This significant increase can be attributed to rapid urbanization, expansion of impervious surfaces such as concrete and asphalt, and the replacement of vegetated areas with infrastructure. Urban heat island effects further intensify surface temperatures in built-up regions.

Vegetation areas also experienced an increase in LST, rising by 4.05°C from 1990 to 2007 and 7.28°C from 2007 to 2024. Although vegetated areas generally help regulate temperatures through evapotranspiration, the observed increase suggests a decline in vegetation cover or degradation of green spaces. Deforestation and land-use changes may have contributed to this temperature rise, emphasizing the need for afforestation and conservation efforts.

Water bodies, which generally exhibit more stable temperatures, showed a relatively smaller increase compared to other land cover types. The temperature of water bodies rose by 2.33°C from 1990 to 2007 and by 3.70°C from 2007 to 2024. The lower rate of increase indicates that water bodies act as thermal buffers, helping to moderate temperature fluctuations. However, rising LST in water bodies may suggest increased evaporation rates, reduced water levels, or changes in hydrological dynamics due to climate variations.

Overall, the increasing LST across all land cover types highlights the impact of land use changes on surface temperature dynamics. The most significant temperature rise was observed in built-up and bare land areas, emphasizing the role of urban expansion and land degradation in driving higher surface temperatures. To mitigate these effects, sustainable land management practices such as urban greening, afforestation, and improved water conservation strategies should be implemented. These measures can help regulate temperatures, enhance environmental resilience, and support sustainable urban development in Bishoftu. Below table provides a clear depiction of temperature variations across different LULC classes in the study area

Table 4.8 Mean Temperature and Changes in Temperature (1990–2024)

	Mean LST (°C)			Change in LST (°C)		
LULC Classes	1990	2007	2024	1990–2007	2007–2024	1990–2024
Agriculture	28.05	29.18	38.85	1.12	9.67	10.79
Bare Land	29.93	31.52	39.06	1.58	9.13	10.72
Built-up	20.47	24.48	34.23	4.01	9.75	13.75
Vegetation	17.64	21.69	28.97	4.045	7.28	11.33
Water	14.65	16.98	20.67	2.33	3.70	6.03

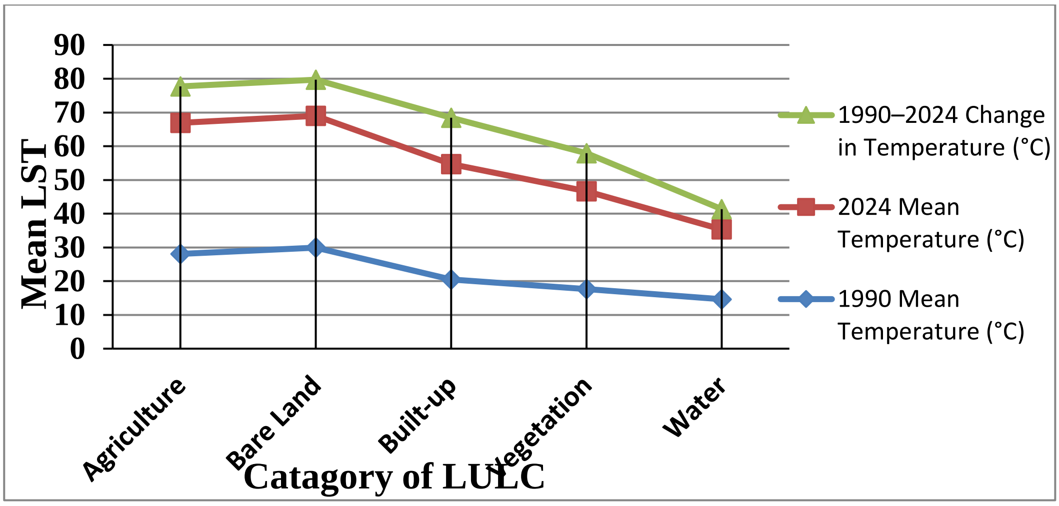

Fig 4.9: Compares the mean LST across the five different LULC zones in Bishoftu during the study period

4.5.2 Urban Area Land Surface Temperature from 1990 to 2024

The analysis of LULC changes over the past 34 years indicates that Bishoftu city has undergone rapid urban expansion, significantly influencing LST. To assess how urbanization has affected LST, the "Extract by Mask" tool in ArcGIS was used to isolate the temperature data for built-up areas. This enabled a focused analysis of temperature variations within the urban environment.

The findings reveal a consistent rise in urban area LST over the study period. In 1990, the LST in built-up areas ranged from 17.62°C to 34.53°C. By 2007, the temperature range had increased slightly to 18.98°C to 36.19°C, reflecting a gradual warming trend. However, by 2024, there was a significant rise in urban temperatures, with LST values ranging from 33.53°C to 47.03°C. This sharp increase suggests that urbanization, infrastructure development, and changes in land cover have intensified heat retention within built-up areas.

Rapid City growth, the expansion of hard surfaces like concrete and asphalt, and the decline in vegetated areas are the main causes of the rise in urban LST. The urban heat island (UHI) effect, which causes built-up areas to have greater temperatures than nearby rural or vegetated areas, is exacerbated by these changes. As illustrated in Table 4.7, the maximum LST in urban areas has significantly increased over time, underscoring the impact of urbanization on surface temperature dynamics.

These results demonstrate how urgently climate adaption and sustainable urban development are needed. The ongoing growth of metropolitan centers could result in additional LST increases if ignored, worsening the problems with the environment and public health.

Table 4.9 Urban Area Land Surface Temperature from 1990 to 2024

Year	Min Temp (°C)	Max Temp (°C)	Mean Temp (°C)	Standard Deviation (°C)
1990	17.62	34.53	25.08	5.62
2007	18.98	36.19	27.56	5.34
2024	33.53	47.03	40.41	4.37

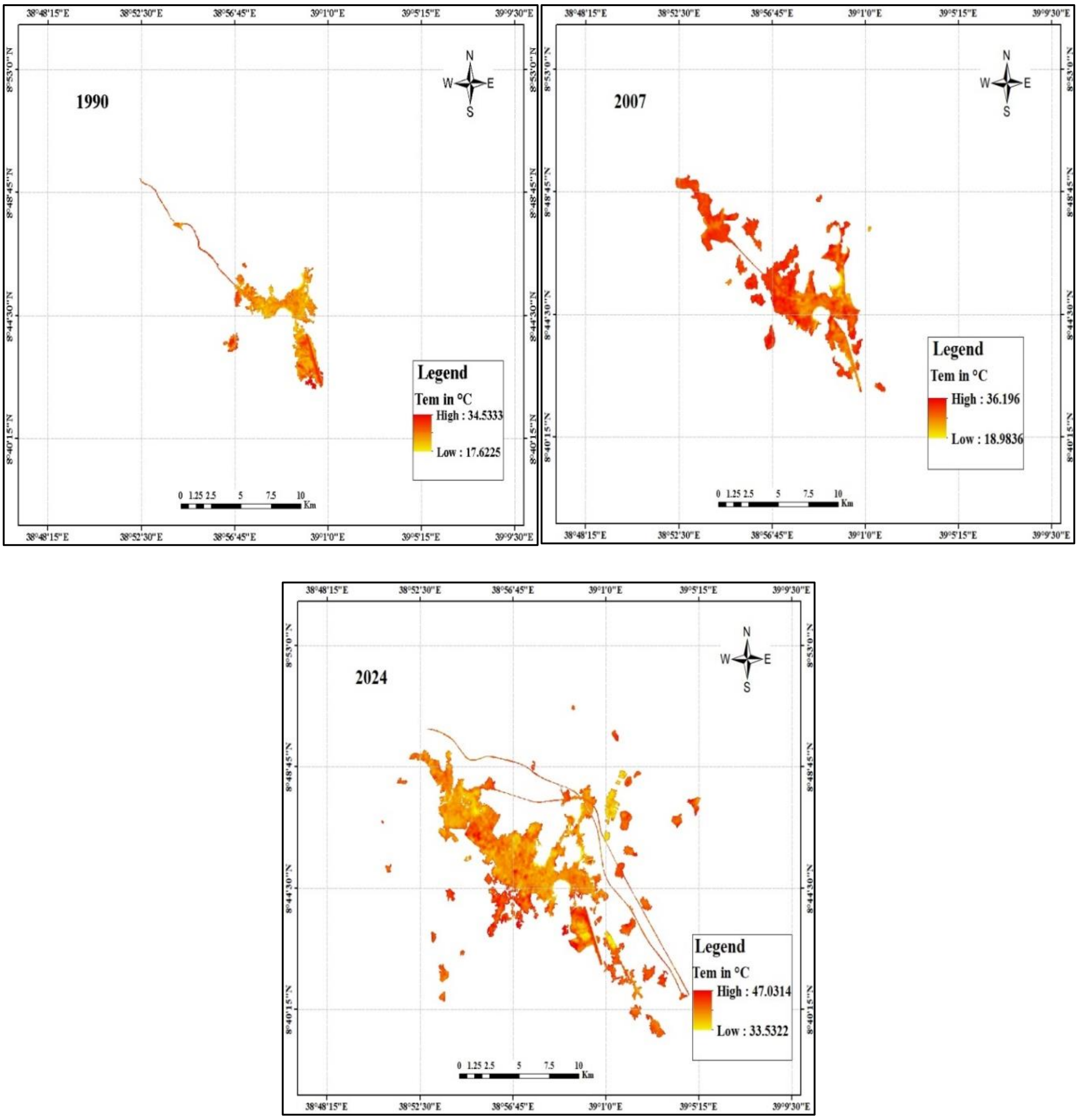

Fig 4.10: Urban Area LST from 1990 to 2024

The LST data for the years 1990, 2007, and 2024 show a noticeable increase in temperature over the years. In 1990, the minimum LST was 17.62°C, while the maximum reached 34.53°C, with a mean of 25.08°C and a standard deviation of 5.62°C. By 2007, the minimum LST had risen to 18.98°C, the maximum to 36.19°C, and the mean to 27.56°C, with a slightly lower standard deviation of 5.34°C. However, by 2024, the minimum LST significantly increased to 33.53°C, and the maximum rose to 47.03°C, resulting in a mean of 40.41°C and a reduced standard deviation of 4.37°C. This indicates a general upward trend in the LST over the three decades.

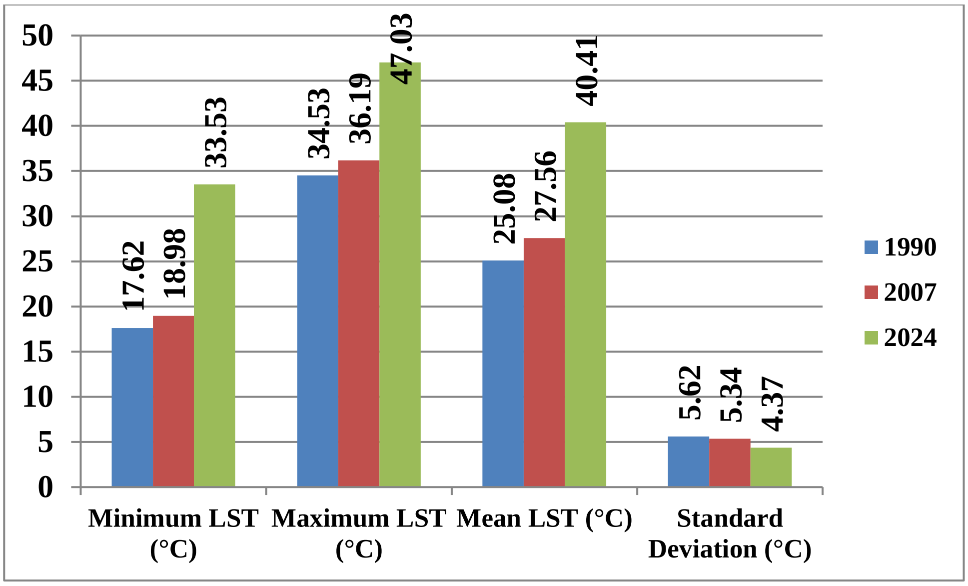

Fig 4.11: Mean LST of urban area between 1990 and 2024

4.5.3 Relationship Between LST and NDVI

The influence of vegetation on the local climate was shown by the important inverse correlation established between the LST and NDVI compared to the nearby rural or vegetated areas. In general, as the NDVI increases, indicating higher vegetation density, the LST tends to decrease, and vice versa. This is primarily due to processes such as transpiration and evapotranspiration, in which vegetation helps cool the surrounding environment (Shahfahad et al., 2020). The analysis of LST and NDVI for 1990, 2007, and 2024 in the study area supports this inverse relationship.

The NDVI values changed over time, with the minimum NDVI values ranging from -0.421 in 1990 to -0.184 in 2024, while the maximum NDVI values remained relatively stable, from 0.607 in 1990 to 0.418 in 2024. The mean NDVI was 0.093 in 1990, 0.1605, in 2007, and 0.117 in 2024, reflecting an overall slight increase in vegetation during 1990–2007 followed by a small decrease in 2024. The standard deviation of NDVI decreased from 0.2968 in 1990 to 0.1738 in 2024, indicating a reduction in the variability of vegetation across the study area.

The LULC class data reveal significant land-use changes, particularly in agricultural, bare land, and built-up areas. Agricultural land decreased over the three decades, while built-up areas expanded significantly, especially between 2007 and 2024. This shift likely contributed to the observed increase in LST, as urbanization and the reduction of vegetated areas can elevate surface temperatures (Gebrekidan et al., 2021).

The inverse relationship between LST and NDVI observed here is consistent with findings from other studies (Gebrekidan et al., 2021; Shahfahad et al., 2020), as well as urban studies by Jiang et al. (2017), which also reported a negative correlation between LST and NDVI, indicating that areas with more vegetation typically experience cooler surface temperatures. As vegetation cover decreases due to urban expansion and land conversion (e.g., agriculture and built-up areas), LST tends to rise, highlighting the crucial role of vegetation in regulating land surface temperature.

A convincing story of the interaction between vegetation and temperature dynamics over time can be told from the R^2 values derived from the examination of the relationship between LST and the NDVI for the years 1990, 2007, and 2024. With an R^2 value of 0.9441 in 1990, the correlation is extraordinarily strong, indicating that variations in NDVI account for roughly 94.41% of the fluctuation in LST. This strong link might be the result of a time when vegetation and land use patterns were comparatively stable and natural ecosystems had a significant impact on surface temperatures. The strong correlation seen this year emphasizes how important vegetation is in regulating regional climates through processes like evapotranspiration and shade.

Even while the connection is still significant, the R^2 value drops slightly to 0.9216 when we go on to 2007, meaning that NDVI still accounts for about 92.16% of the variability in LST. This slight decrease might be an indication of new land cover changes that are starting to take shape, either as a result of growing urbanization, agricultural growth, or altered climatic patterns that have already started to impact the terrain. The decrease in explanatory power raises the possibility that over this time, variables other than vegetation, such as soil moisture content, human activity, and climate variability, began to have a greater impact on surface temperatures. However, the link is still strong, suggesting that despite these changes, vegetation still has a considerable impact on LST.

It's interesting to note that the R^2 value for 2024 increases to 0.9343 once more, indicating that the correlation between LST and NDVI is becoming stronger. This increase would suggest that adaptive responses in land use or vegetation management have strengthened the link between vegetation and temperature, even in the face of pressures from urbanization or climate change. It poses fascinating queries about whether specific tactics have been used to increase vegetation cover as a way to mitigate climate change and how ecosystems may be reacting to shifting climatic conditions. The fact that a large association has persisted in this more recent year shows how important vegetation is still in controlling local temperatures and implies that tracking these relationships is still essential to comprehending ecological resilience and health.

The results suggest that increasing urbanization and changes in land use/land cover, particularly the expansion of built-up areas, are likely contributing to the observed increase in LST in the study area, which is consistent with the inverse relationship between NDVI and LST (Jiang et al., 2017).

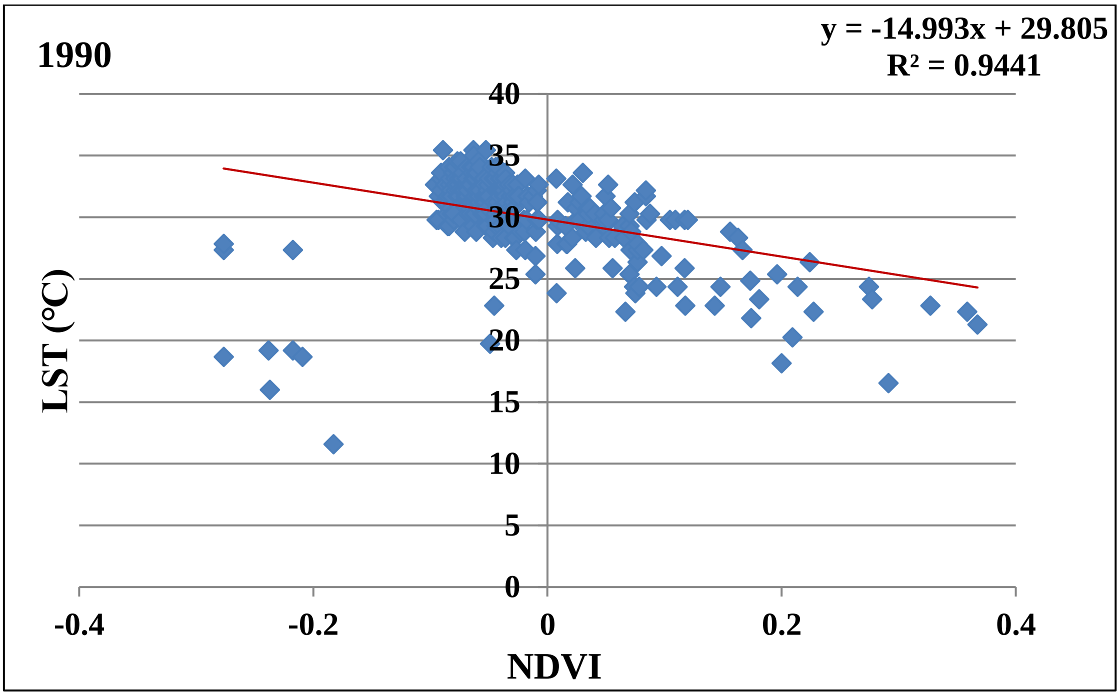

Fig 4.12: Correlation between LST and NDVI within 1990

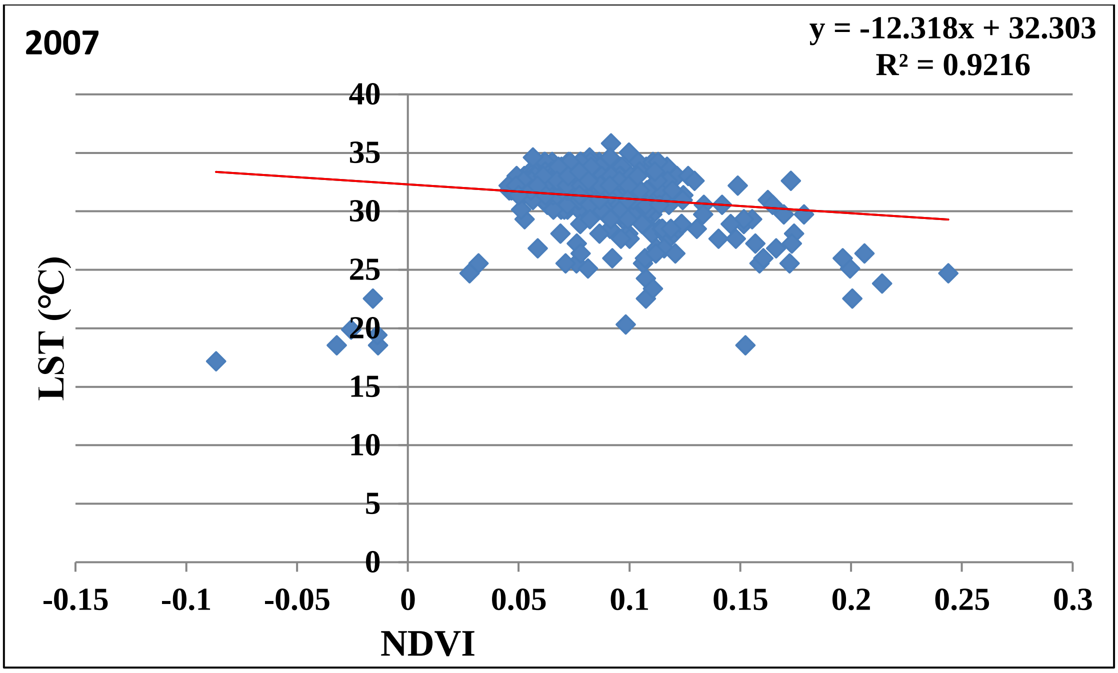

Fig 4.13: Correlation between LST and NDVI within 2007

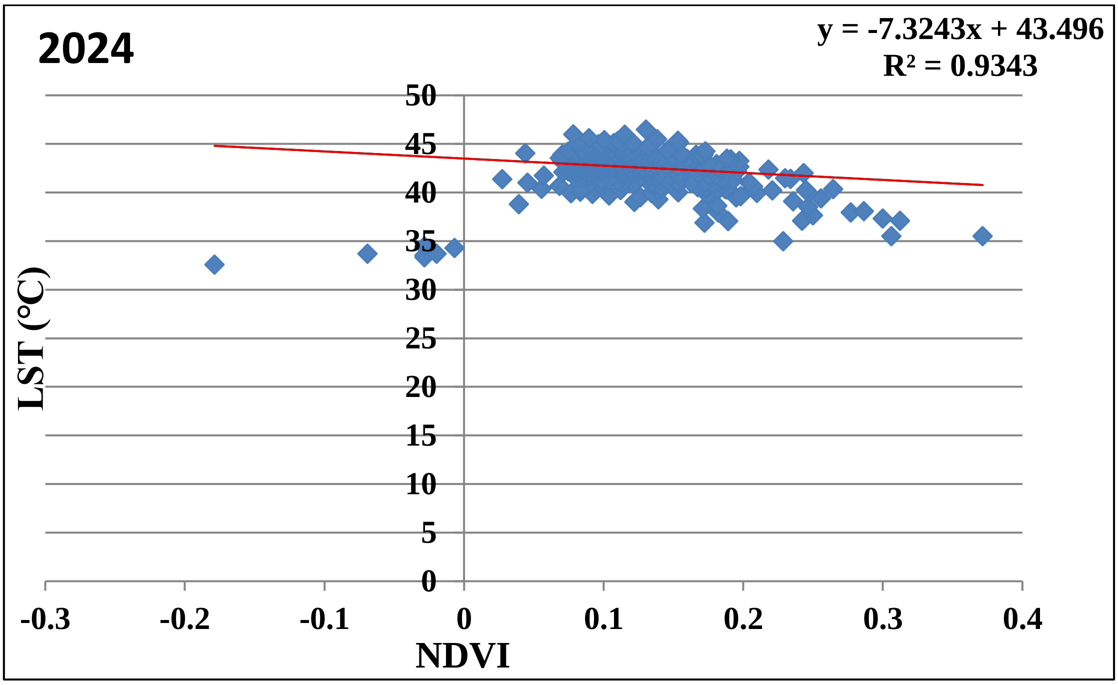

Fig 4.14: Relationship between LST & NDVI within 2022

4.5.4 Relationship between LST & NDBI

Understanding the urban heat island (UHI) effect and its effects on urban climates depends critically on the link between LST and NDBI. The local climate is significantly impacted by the conversion of natural land cover to built-up areas as urbanization advances, especially through the raising of surface temperatures. This section examines the correlation between

LST and NDBI in Bishoftu city from 1990 to 2024, providing insights into how urban growth has influenced temperature variations across the city.

Temporal Trends in LST and NDBI

Over the three decades analyzed, both LST and NDBI show a clear upward trend, suggesting a positive relationship between urban expansions and rising surface temperatures. As illustrated in the analysis, the NDBI values for Bishoftu city shifted from -0.281 in 1990 to -0.594 in 2024, reflecting a significant increase in built-up areas. This shift is accompanied by a marked rise in LST, with temperatures in urban areas rising from 34.53°C in 1990 to 47.03°C in 2024. The consistent rise in both NDBI and LST indicates a strong connection between the expansion of built-up areas and the increase in surface temperatures.

The NDBI-LST Correlation

The mechanism of the urban heat island (UHI) effect can be used to understand the relationship between NDBI and LST. Natural vegetation is being replaced by impervious surfaces like asphalt roads, concrete structures, and rooftops as urban areas grow. These materials absorb and retain heat, thereby increasing the surface temperature. The NDBI, which measures the contrast between built-up and non-built-up areas, shows higher values as urbanization intensifies, indicating the growing dominance of built-up surfaces over natural land cover. Consequently, the increase in NDBI correlates with rising LST values, highlighting the effect of urban growth on local temperature dynamics.

In 1990, the NDBI values were low, reflecting minimal urban development and consequently lower LST. However, as urban areas expanded, NDBI values increased, and this was mirrored by an increase in LST, particularly between 2007 and 2024. The rise in NDBI from -0.317 in 2007 to -0.594 in 2024 corresponds with an increase in the maximum LST from 36.19°C in 2007 to 47.03°C in 2024. This positive relationship confirms that the spread of built-up areas is directly contributing to the rise in urban temperatures, reinforcing the UHI effect.

Environmental Implications of the NDBI-LST Relationship

The positive relationship between NDBI and LST has significant environmental implications for Bishoftu city. The UHI effect is made increasing by the growing impermeable surfaces in built-up areas, which raises temperatures in urban areas relative to nearby rural areas. This may results in a number of negative effects, such as higher air pollution levels, more energy being used for cooling, and a higher chance of heat-related illnesses. Additionally, the rise in LST may alter local weather patterns, impact water resources, and reduce biodiversity, as urban expansion displaces natural habitats.

Urban Planning and Mitigation Strategies

In order to create sustainable urban planning methods that lessen the UHI effect and its related effects, it is essential to comprehend the relationship between LST and NDBI. To counteract the increasing LST, urban planners should focus on enhancing green infrastructure, such as the creation of urban parks, the promotion of rooftop gardens, and the expansion of tree cover. These measures would not only help lower surface temperatures but also improve air quality and overall urban livability. Furthermore, using heat-reflective materials in urban construction and incorporating green spaces into new developments can reduce the absorption of heat by built-up areas, helping to maintain more balanced temperature conditions.

4.5.5 Relationship between Urban Expansion and Urban LST

The conversion of natural land covers into impermeable surfaces like buildings, highways, and industrial areas is the main reason why urban expansion has a significant effect on the LST. The rapid urbanization of Bishoftu city between 1990 and 2024 has resulted in significant LULC changes, leading to a marked increase in surface temperatures. As built-up areas expanded from 15.59 km² (2.87% of the total land area) in 1990 to 69.90 km² (12.89%) in 2024, the LST of urban regions also showed a consistent upward trend. In 1990, the LST in built-up areas ranged from 17.62°C to 34.53°C, while in 2007, it increased to a range of 18.98°C to 36.19°C. By 2024, urban temperatures had risen significantly, with LST values ranging from 33.53°C to 47.03°C. The mean temperature of the urban areas also followed a similar trend, increasing from 25.08°C in 1990 to 40.41°C in 2024, indicating a strong positive correlation between the urban expansion and LST rise.

One of the primary drivers of this temperature increase is the loss of vegetation and its associated cooling effects. By evapotranspiration and shade, vegetation is essential for controlling surface temperatures. However, as natural landscapes are replaced by urban infrastructure, the cooling benefits of vegetation diminish, leading to higher surface temperatures. This study's NDVI analysis confirmed a consistent decline in vegetation cover over the study period, reinforcing the inverse relationship between green spaces and LST. In contrast, the NDBI values increased steadily, indicating the expansion of the built-up areas, which directly contributed to the rise in surface temperatures.

Another key factor contributing to the urban LST rise is the increase in impervious surfaces, which absorb and retain more heat than natural land covers. Materials such as asphalt, concrete, and rooftops have lower albedo and higher thermal inertia, leading to greater heat accumulation during the day and slower heat dissipation at night. The urban heat island (UHI) effect is a phenomenon that causes urban areas to be noticeably warmer than the rural areas around them. The spatial distribution of LST in Bishoftu reveals that the highest temperatures are concentrated in densely built-up areas, whereas lower temperatures are recorded in less urbanized and vegetated regions.

In addition to changes in land cover, human activities associated with urban expansion contribute to the rising temperatures. Increased energy consumption for residential, commercial, and industrial activities generates excess heat, further intensifying local temperature variations. Furthermore, urban density plays a significant role in temperature variability, with densely built-up areas experiencing higher LST than sparsely developed regions. The results of this study align with previous research conducted in rapidly urbanizing cities worldwide (Jiang et al., 2017; Shahfahad et al., 2020), which also found a strong positive correlation between urban expansion and LST rise.

The implications of these findings are critical to urban planning and environmental sustainability. Rising urban temperatures can lead to increased cooling energy demand, increased heat stress, and changes in local climates. To mitigate these effects, urban development policies should integrate climate-sensitive planning approaches. This includes increasing vegetation cover through afforestation and reforestation initiatives, using heat-reflective building materials, implementing urban greening projects, and promoting sustainable land management practices. Implementing zoning regulations that promote dense urban development while protecting green spaces can help reduce rising urban land surface temperatures.

A phenomenon known as the urban heat island (UHI) effect makes cities notably warmer than the surrounding rural areas.

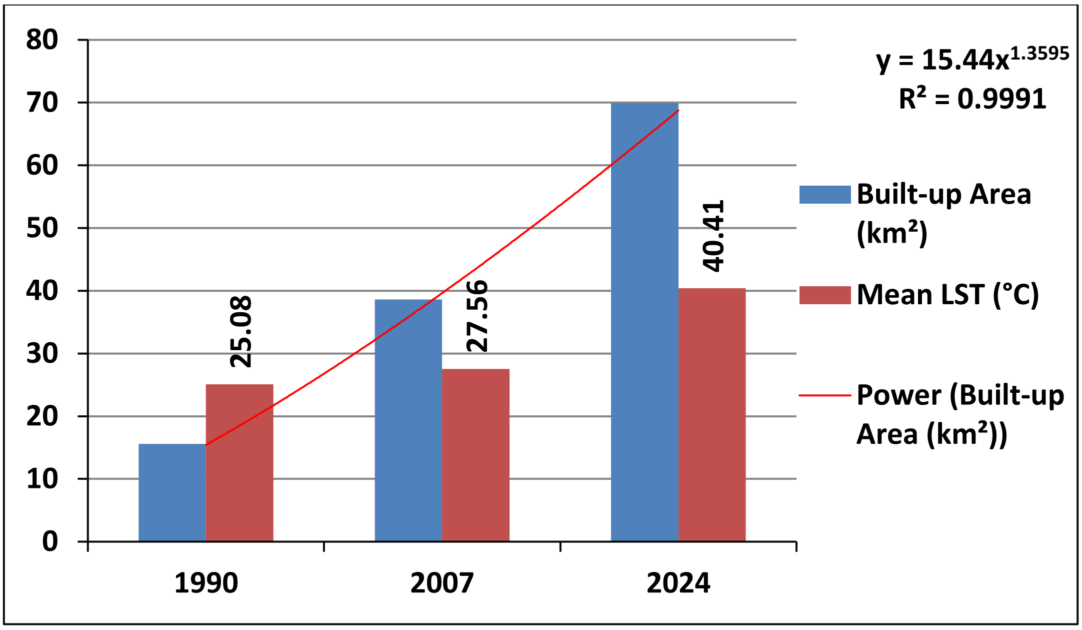

Fig 4.15: Relationship between Urban Expansion and Urban LST

4.5.6 Validation of the result for land surface temperature

To perform any type of additional analysis, the recovered LST must be validated using Landsat data with in situ measurement or with any other satellite data. Due to the unavailability of in situ measurement, Moderate Resolution Imaging Spectroradiometer (MODIS) satellite data were applied as a reference image for the validation of LST retrieved from Landsat data (Emami & Rahmanizadeh, 2022; Guillevicet al., 2018).On a given date, the same study region could not be photographed by MODIS and Landsat sensors. As a result, MODIS data acquisition dates were either one day before or one day after Landsat data acquisition dates. During the selected satellite picture acquisition dates for both sensors, no air disturbances were detected. The recovered LST had a spatial resolution of 1000 m for MODIS data and 100 m for Landsat data. In order to match the Landsat products, the MODIS LSTs were resampled to 100m prior to data comparison. The Landsat mean LST and the matching MODIS mean LST values were found to deviate by a little amount (3.39 °C). Discrepancies between MODIS and Landsat LST is due to the 30-minute intervals between the Landsat 8 and MODIS sensors, the water vapor content, and the scale effect in the resampling method (Subhanil et al. 2019). The 30-minute interval between Landsat 8 and MODIS overpasses means that the sensors capture surface temperatures at slightly different times, which can lead to variations due to diurnal temperature fluctuations. During this period, surface temperatures may rise or fall depending on weather conditions, solar radiation, and land cover characteristics, resulting in discrepancies when comparing the datasets. Water vapor content in the atmosphere also plays a critical role, as higher humidity levels can absorb and scatter thermal infrared radiation differently, affecting the accuracy of LST retrievals from both sensors. Variations in atmospheric water vapor can lead to differences in the thermal signal, especially if atmospheric corrections are not uniformly applied. Additionally, the process of resampling data to match spatial resolutions introduces a scale effect; methods such as bilinear or cubic convolution can smooth or alter the thermal signals, potentially causing mismatches between the high-resolution Landsat data and the coarser MODIS observations. Together, these factors contribute to the observed discrepancies.

4.6 Discussion

This section examines the key findings regarding alterations in LULC, vegetation dynamics, the expansion of built-up areas, and fluctuations in LST in Bishoftu city from 1990 to 2024. The results are contextualized by comparing them with previous studies, discussing their implications, addressing limitations, and suggesting directions for future research.

4.6.1 LULC Changes in Bishoftu city

The study reveals substantial LULC transformations, primarily characterized by rapid urban expansion and a concurrent reduction in agricultural land and vegetation cover. The built-up area increased from 15.59 km² in 1990 to 69.90 km² in 2024, representing a 348.45% growth, while agricultural and vegetative land decreased proportionally. These findings align with studies in other rapidly urbanizing cities, such as Addis Ababa (Belay & Mengistu, 2021) and Nairobi (Mundia & Aniya, 2020), where similar urban expansion trends have been reported.

The expansion of built-up areas is primarily driven by population growth, infrastructure development, and increased housing demand, leading to the encroachment of agricultural lands. This transformation has significant implications for food security and ecological stability. Gebrehiwot et al. (2022) highlighted similar concerns, emphasizing that uncontrolled urbanization disrupts microclimates, biodiversity, and land productivity. The findings underscore the need for integrated urban planning that balances development with environmental conservation.

4.6.2 Changes in Vegetation Cover: NDVI Analysis

NDVI analysis indicates a declining trend in vegetation cover, with the mean NDVI decreasing from 0.093 in 1990 to 0.117 in 2024. This reduction in vegetation is associated with urban sprawl and land-use conversion, which is consistent with findings from Abebe et al. (2023) in Ethiopia and Jiang et al. (2019) in China, where rapid urbanization has led to deforestation and the loss of green spaces.

Vegetation plays a crucial role in regulating LST through evapotranspiration and carbon sequestration. The observed decline in NDVI suggests adverse effects on local climatic conditions, including increased surface temperatures and deteriorating air quality. Shahfahad et al. (2020) reported that declining NDVI values in urban areas correlate with rising LST, reinforcing the importance of urban greenery. This study highlights the need for afforestation initiatives, green infrastructure, and conservation efforts to mitigate the environmental consequences of urban expansion.

4.6.3 Expansion of Built-Up Areas: NDBI Analysis

The NDBI analysis shows a steady increase in built-up areas, reflecting continuous urban expansion. The shift from a relatively low NDBI value in 1990 to significantly higher values in 2024 is consistent with studies conducted in Africa (Hassan et al., 2021) and Asia (Liu & Weng, 2022), where similar patterns of urbanization and land transformation have been observed.

The rise in NDBI values correlates with a decline in vegetation and agricultural land, illustrating the inverse relationship between urban growth and natural land cover. Increased built-up areas contribute to higher surface runoff, reduced groundwater recharge, and the intensification of urban heat island (UHI) effects. Xu et al. (2023) highlighted that impervious surface exacerbate these environmental impacts, necessitating the adoption of green infrastructure, land-use zoning policies, and sustainable urban development strategies.

4.6.4 Land Surface Temperature (LST) Trends

Maximum LST values in Bishoftu city increased from 38°C in 1990 to 43°C in 2024, indicating a notable warming trend, according to LST study. The highest temperatures are found in urbanized regions, indicating a strong relationship between LST and urban growth. Similar trends have been reported in Lagos (Adeyemi et al., 2020) and Mumbai (Jiang et al., 2017), where urbanization-induced LST increases have intensified UHI effects.

The rise in LST is attributed to the loss of vegetation and an increase in impervious surfaces, leading to altered local microclimates. Studies by Gebrekidan et al. (2021) and Govind & Ramesh (2019) confirm that urban expansion exacerbates temperature intensification, posing challenges for climate resilience. The findings underscore the need for climate adaptation strategies such as green roofs, urban tree planting, reflective building materials, and sustainable urban designs to counteract rising temperatures.

4.6.5 Implications of Findings

The paper emphasizes how Bishoftu city's land-use dynamics and LST are significantly impacted by urban expansion. These results highlight the significance of sustainable land management and are in line with trends in global urbanization. The key implications include:

- Urban Planning: According to the results, sustainable urban expansion methods that incorporate green infrastructure and preserve natural landscapes are essential.
- Climate Mitigation: The rising LST values call for urgent climate adaptation measures to reduce UHI effects.
- Biodiversity Conservation: The loss of vegetation underscores the importance of conservation programs to maintain ecological balance and urban resilience.
- Water Resource Management: Changes in LULC can alter hydrological cycles, necessitating integrated water management approaches.

4.6.6 Study Limitations and Future Research Directions

While this study provides comprehensive insights into LULC changes, NDVI, NDBI, and LST trends, certain limitations must be acknowledged:

- Data Availability: The analysis used 16-day-spaced Landsat pictures, which might not have captured recent changes in land use.
- Climate Factors: External climatic influences, such as rainfall variability and atmospheric conditions, were not explicitly considered in the LST analysis.
- Policy Analysis: While urban expansion trends were analyzed, specific policy interventions impacting LULC changes were not examined in depth.

Future research should focus on:

a. Utilizing High-Resolution Satellite Imagery and Advanced Remote Sensing Techniques

Future research should employ high-resolution satellite imagery and improved remote sensing technologies to boost the accuracy of LULC and LST assessments. This would improve the spatial and temporal resolution of monitoring urban expansion and temperature changes, offering more detailed insights into urban heat islands and environmental impacts.

b. Investigating Socio-Economic and Policy Influences on Urban Expansion Future research should explore how socio-economic factors, such as population growth, economic development, and governance policies, influence urban expansion and land-use changes. Understanding these drivers can inform sustainable urban planning, policy interventions, and the management of urban growth in rapidly developing regions.

c. Evaluating the Long-Term Effects of Urbanization on Biodiversity and Ecosystem Services

   Investigating the long-term effects of urbanization on ecosystem services and biodiversity is crucial. Future studies should focus on how urban expansion alters ecosystems, disrupts natural habitats, and affects biodiversity, providing a foundation for conservation strategies and ensuring the resilience of urban ecosystems.

d. Development of Predictive Models for Future LULC and Temperature Trends developing predictive models to forecast future land-use and temperature changes under different urban planning scenarios is essential. These models can guide decision-makers in creating effective urban planning policies that mitigate the adverse effects of urbanization, such as elevated land surface temperatures and loss of green spaces.

5. CONCLUSION AND RECOMMENDATIONS

5.1 Conclusion

The results of this study unequivocally demonstrate that rapid urbanization in Bishoftu City has significantly altered LULC patterns, leading to an increase in LST over the past three decades. The most striking transformation was the expansion of the built-up areas, which increased from 15.59 km² in 1990 to 69.90 km² in 2024, representing a 348.45% growth. This expansion primarily replaced agricultural land and vegetative cover, intensifying surface temperature rise and contributing to localized urban heat island (UHI) effects.

Each the positive relationship between NDBI and LST and the negative link between NDVI and LST reflect the major effect of built-up regions on temperature intensification, while the latter highlights the vital role of vegetation in reducing urban heat. These findings are consistent with those of previous studies (Jiang et al., 2017; Shahfahad et al., 2020), which have also reported that urbanization exacerbates heat accumulation, alters microclimates, and heightens UHI effects.

By providing empirical evidence of LULC-driven temperature changes in a rapidly urbanizing city, this study contributes to the growing body of literature on urban remote sensing. The results emphasize the urgent need to integrate environmental sustainability into urban planning to enhance long-term resilience against climate change.

5.2 Summary

This study used remote sensing and GIS-based methods to evaluate how urban growth affected the LST in Bishoftu city between 1990 and 2024. Analyzing LULC changes, examining the connection between LST and spectral indices such the NDVI and NDBI, and assessing the wider environmental effects of urbanization were the main objectives of the study.

Most significant LULC transitions were found, as evidenced by the large growth in built-up areas at the expense of agricultural land and vegetation. Over the course of the study, NDVI analysis showed a steady decrease in plant cover, which helped to raise LST. Conversely, NDBI values demonstrated a steady rise, highlighting rapid urban expansion. The study found an inverse relationship between NDVI and LST, indicating that while highly urbanized regions had higher LST, locations with more vegetation cover had lower surface temperatures. These findings highlight the necessity of climate adaptation plans and sustainable urban planning in order to lessen the negative environmental effects of urbanization.

5.3 Recommendations

The following suggestions are put out in light of the study's findings to solve the issues raised by Bishoftu city's urban growth and rising LST:

- ✓ Sustainable urban planning and green infrastructure development policymakers and urban planners should incorporate sustainable urban design principles that prioritize green spaces, tree planting, and vegetative buffers. Implementing urban parks, green roofs, and vertical gardens can help mitigate rising temperatures and reduce UHI effects.
- ✓ Strengthening land-use policies and regulations local authorities should establish and enforce land-use policies that promote controlled urban expansion while preserving natural ecosystems. Climate-sensitive urban development strategies should be integrated into city planning to minimize the adverse effects of built-up areas on LST.
- ✓ Enhanced remote sensing and GIS-based monitoring regular and systematic monitoring of LULC and LST changes should be conducted using advanced remote sensing and GIS technologies. This approach will provide accurate, real-time data for decision-making and urban planning, enabling proactive interventions to address urban heat challenges.
- ✓ Afforestation and reforestation initiatives large-scale afforestation and reforestation programs should be promoted to counteract the loss of vegetation due to urban expansion. Urban tree planting campaigns, particularly in high-temperature zones, can significantly contribute to moderating surface temperatures.
- ✓ Climate-resilient building materials and designs the construction sector should adopt energy-efficient and climate-resilient building materials that minimize heat absorption. The use of reflective roofing, cool pavements, and improved ventilation systems can help reduce urban heat and enhance livability.
- ✓ Further research is needed to examine the long-term and seasonal impacts of urban expansion on land surface temperature, and community awareness campaigns should be launched to promote sustainable urban practices.

References

Abebe, B., Tsegaye, D., & Tesfaye, G. (2023). Urbanization and its impact on vegetation dynamics in Ethiopian cities: A case study of Addis Ababa. Environmental Monitoring and Assessment, 195(5), 348.

Achmad, A., Fadhly, N., Deli, A., & Ramli, I. (2022). Urban growth and its impact on land surface temperature in an industrial city in Aceh, Indonesia. Letters in Spatial and Resource Sciences, 15(1), 39–58.

Alemu, M. M. (2019). Analysis of spatio-temporal land surface temperature and normalized difference vegetation index changes in the Andassa watershed, Blue Nile Basin, Ethiopia. Journal of Resources and Ecology, 10(1), 77–85. https://doi.org/10.5814/j.issn.1674-764X.2019.01.010

Alliance, C. (2015). The Ethiopia Urbanization Review: Urban Institutions for a Middle Income. The World Bank Group. https://openknowledge.worldbank.org/handle

Attri, P., Chaudhry, S., & Sharma, S. (2015). Remote sensing & GIS-based approaches for LULC change detection–A review. International Journal of Current Engineering and Technology, 5, 3126–3137.

Avis, W. R. (2019). Urban expansion in Nigeria.

Ayanlade, A., Aigbiremolen, M. I., & Oladosu, O. R. (2021). Variations in urban land surface temperature intensity over four cities in different ecological zones. Scientific Reports, 11(1), 1–17.

Bao, T., Li, X., & Zhang, J. (2016). Assessing the distribution of urban green spaces and its anisotropic cooling distance on urban heat island pattern in Baotou, China. ISPRS International Journal of Geo-Information, 5(2), 12. https://doi.org/10.3390/ijgi5020012

Baqa, M. F., Lu, L., Chen, F., Nawaz-ul-Huda, S., Pan, L., Tariq, A., & Li, Q. (2022). Characterizing spatiotemporal variations in the urban thermal environment related to land cover changes in Karachi, Pakistan, from 2000 to 2020. Remote Sensing, 14(9), 2164.

Bezerra, P. E., Moraes, E. T., & Soares, I. R. (2018). Analysis of surface temperature and vegetation index in the municipality of Belém in identification of the heat islands. Revista Brasileira de Cartografia, 70, 803–818.

Belay, D., & Mengistu, A. (2021). Urban growth and land-use change in Addis Ababa: Trends, impacts, and challenges. Urban Studies, 58(4), 561–578.

Bulti, D. T., & Abebe, B. G. (2020). Analyzing the impacts of urbanization on runoff characteristics in Adama city, Ethiopia. SN Applied Sciences, 2(7), 1–13.

Burrough, P. A. (1990). Principles of Geographic Information Systems. Oxford University Press.

Camagni, R., Gibelli, M. C., & Rigamonti, P. (2002). Urban mobility and urban form: The social and environmental costs of different patterns of urban expansion. Ecological Economics, 40(2), 199–216.

Chaithanya, V., Binoy, B., & Vinod, T. (2017). Estimation of the relationship between urban vegetation and land surface temperature of Calicut City and suburbs, Kerala, India using GIS and remote sensing data. International Journal of Advanced Remote Sensing and GIS, 6(1), 2088–2096.

Chao, Z., Wang, L., Che, M., & Hou, S. (2020). Effects of different urbanization levels on land surface temperature change: Taking Tokyo and Shanghai for example. Remote Sensing, 12(12), 2022.

Chen, C., He, X., Liu, Z., Sun, W., Dong, H., & Chu, Y. (2020). Analysis of regional economic development based on land use and land cover change information derived from Landsat imagery. Scientific Reports, 10(1), 1–16.

Chen, Y. C., Chiu, H. W., Su, Y. F., Wu, Y. C., & Cheng, K. S. (2017). Does urbanization increase diurnal land surface temperature variation? Evidence and implications. Landscape and Urban Planning, 157, 247–258.

Choi, Y. Y., Suh, M. S., & Park, K. H. (2014). Assessment of surface urban heat islands over three megacities in East Asia using land surface temperature data retrieved from COMS. Remote Sensing, 6(6), 5852–5867.

Coppin, P. R., & Bauer, M. E. (1996). Digital change detection in forest ecosystems with remote sensing imagery. Remote Sensing Reviews, 13(3–4), 207–234.

Damen, M. (2022). Introduction to Remote Sensing.

Das, D. N., Chakraborti, S., Saha, G., Banerjee, A., & Singh, D. (2020). Analysing the dynamic relationship of land surface temperature and land use pattern: A city level analysis of two climatic regions in India. City and Environment Interactions, 8, 100046. https://doi.org/10.1016/j.cacint.2020.100046

Deb, D., Singh, A. K., & Kumar, S. (2018). Remote sensing techniques in horticulture. In Global Hi-Tech Horticulture (pp. 39–48).

Deng, Y., Wang, S., Bai, X., Tian, Y., Wu, L., Xiao, J., & Qian, Q. (2018). Relationship among land surface temperature and LUCC, NDVI in typical karst area. Scientific Reports, 8(1), 1–12.

Di Gregorio, A. (2005). Land Cover Classification System: Classification Concepts and User Manual (LCCS) (Vol. 2). Food & Agriculture Organization.

Dissanayake, D. M. S. L. B., Morimoto, T., Murayama, Y., & Ranagalage, M. (2019). Impact of landscape structure on the variation of land surface temperature in Sub-Saharan region: A case study of Addis Ababa using Landsat data (1986–2016). Sustainability, 11(8), 2257.

Ebrahimy, H., Aghighi, H., Azadbakht, M., Amani, M., Mahdavi, S., & Matkan, A. A. (2021). Downscaling MODIS land surface temperature product using an adaptive random forest regression method and Google Earth Engine for a 19-years spatiotemporal trend analysis over Iran. IEEE Journal of Selected Topics in Applied Earth Observations and Remote Sensing, 14, 2103–2112. https://doi.org/10.1109/JSTARS.2021.3051422

Estoque, R. C., Murayama, Y., & Myint, S. W. (2016). Effects of landscape composition and pattern on land surface temperature: An urban heat island study in the megacities of Southeast Asia. Science of the Total Environment, 577, 349–359. https://doi.org/10.1016/j.scitotenv.2016.10.195

Foody, G. M. (2002). Status of land cover classification accuracy assessment. Remote Sensing of Environment, 80(1), 185–201.

Gao, J., & O'Neill, B. C. (2020). Mapping global urban land for the 21st century with data-driven simulations and Shared Socioeconomic Pathways. Nature Communications, 11(1), 1–10.

Gebrehiwot, K., Ayalew, A., & Teshome, S. (2022). Urbanization-driven land-use/land-cover changes and their effects on microclimates: A case study of Mekelle. Journal of Environmental Science & Policy, 63(7), 1234–1246.

Gebrekidan, W., Ermias, T., & Amare, B. (2021). Assessing the effects of vegetation change on urban land surface temperature using remote sensing data: The case of Addis Ababa City, Ethiopia. Remote Sensing Applications: Society and Environment, 22, 100520.

Govind, N. R., & Ramesh, H. (2019). The impact of spatiotemporal patterns of land use land cover and land surface temperature on an urban cool island: A case study of Bengaluru. Environmental Monitoring and Assessment, 191, 1–20.

Grover, A., & Singh, R. (2016). Monitoring spatial patterns of land surface temperature and urban heat island for sustainable megacity: A case study of Mumbai, India using Landsat TM data. Environment and Urbanization Asia, 7(1), 38–54. https://doi.org/10.1177/0975425315619722

Hassan, M. I., Oyinloye, M. A., & Olalekan, O. (2021). Urban expansion and its impact on land use in African cities: A remote sensing analysis. Journal of Urban Planning and Development, 147(3), 04021034.

Hashim, B. M., Al Maliki, A., Sultan, M. A., Shahid, S., & Yaseen, Z. M. (2022). Effect of land use land cover changes on land surface temperature during 1984–2020: A case study of Baghdad city using landsat image. *Natural Hazards*, *112*(2), 1223-1246.

Huang, S., Tang, L., Hupy, J. P., Wang, Y., & Shao, G. (2021). A commentary review on the use of normalized difference vegetation index (NDVI) in the era of popular remote sensing. Journal of Forestry Research, 32(1), 1-6.

Huang, C., Zhang, S., & Li, Y. (2020). Remote sensing monitoring of urban vegetation and its implications for urban sustainability. Remote Sensing of Environment, 239, 111629.

Ibitoye, M. O., Aderibigbe, O. G., Adegboyega, S. A., & Adebola, A. O. (2017). Spatiotemporal analysis of land surface temperature variations in the rapidly developing Akure and its environs, southwestern Nigeria using Landsat data. Ethiopian Journal of Environmental Studies and Management, 10(3), 389–403.

Imran, H. M., Hossain, A., Islam, A. S., Rahman, A., Bhuiyan, M. A. E., Paul, S., & Alam, A. (2021). Impact of land cover changes on land surface temperature and human thermal comfort in Dhaka City of Bangladesh. Earth Systems and Environment, 1–27.

Islam, A. S., Islam, G. T., & Roy, D. (2021). An analysis of spatio-temporal trends of land surface temperature in the Dhaka metropolitan area by applying landsat images. (No Journal provided, please double-check this citation)

Javed, T., Li, Y., Feng, K., Ayantobo, O. O., Ahmad, S., Chen, X., & Suon, S. (2021). Monitoring responses of vegetation phenology and productivity to extreme climatic conditions using remote sensing across different sub-regions of China. Environmental Science and Pollution Research, 28(3), 3644–3659.

Jiang, T. B., Deng, Z. W., Zhi, Y. P., Cheng, H., & Gao, Q. (2021). The effect of urbanization on population health: Evidence from China. Frontiers in Public Health, 766.

Jiang, X., Zhang, Y., & Xu, H. (2019). Urban expansion and its impact on land cover change in China: A satellite-based analysis. Landscape and Urban Planning, 187, 94–104. https://doi.org/10.1016/j.landurbplan.2019.01.010

Kafy, A. A., Rahman, M. S., Hasan, M. M., & Islam, M. (2020). Modelling future land use land cover changes and their impacts on land surface temperatures in Rajshahi, Bangladesh. Remote Sensing Applications: Society and Environment, 18, 100314.

Kanga, S., Meraj, G., Johnson, B. A., Singh, S. K., PV, M. N., Farooq, M., & Sahu, N. (2022). Understanding the linkage between urban growth and land surface temperature—A case study of Bangalore City, India. Remote Sensing, 14(17), 4241.

Kassouri, Y., & Okunlola, O. A. (2022). Analysis of spatio-temporal drivers and convergence characteristics of urban development in Africa. Land Use Policy, 112, 105868.

Khin, M. Y., Shin, D. Y., Park, J. J., & Choi, C. C. (2012). Land surface temperature changes by LU changes of Inlay Lake area, Myanmar. Department of Spatial Information Engineering, Pukyong National University, South Korea.

Kumari, B., Tayyab, M., Mallick, J., Khan, M. F., & Rahman, A. (2018). Satellite-driven land surface temperature (LST) using Landsat 5, 7 (TM/ETM+ SLC) and Landsat 8 (OLI/TIRS) data and its association with built-up and green cover over urban Delhi, India. Remote Sensing in Earth Systems Sciences, 1(3), 63–78.

Kundu, D., & Pandey, A. K. (2020). World urbanization: Trends and patterns. In Developing National Urban Policies (pp. 13–49). Springer, Singapore.

Li, Z. L., Tang, B. H., Wu, H., Ren, H., Yan, G., Wan, Z., ... & Sobrino, J. A. (2013). Satellite-derived land surface temperature: Current status and perspectives. Remote Sensing of Environment, 131, 14–37.

Liaqut, A., Younes, I., Sadaf, R., & Zafar, H. (2019). Impact of urbanization growth on land surface temperature using remote sensing and GIS: A case study of Gujranwala City, Punjab, Pakistan. International Journal of Economic and Environmental Geology, 44–49.

Liu, X., & Weng, Q. (2022). Spatiotemporal analysis of urbanization and its environmental impacts in Asian megacities. Remote Sensing of Environment, 267, 112738.

Luo, H., & Wu, J. (2021). Effects of urban growth on the land surface temperature: A case study in Taiyuan, China. Environment, Development and Sustainability, 23(7), 10787–10813.

McMillen, D. P., & Smith, S. C. (2003). The number of subcenters in large urban areas. Journal of Urban Economics, 53(3), 321–338.

Merga, B. B., Tabor, K. W., & Alemu, G. (2021). Analysis of the Cooling Effect of Urban Green Spaces in Mitigating Micro-climate Change Using Geospatial Techniques in Adama City, Central Ethiopia.

Mirsanjari, M. M., Mohammadyari, F., Visockiene, J. S., & Zarandian, A. (2021). Relationship between land surface temperature and urbanization in Vilnius district. Environmental Monitoring and Assessment, 193(8), 1–14.

Mitiku, B. M., Indale, N. D., & Dessalegn, O. G. (2022). Integration of geospatial technologies with multiple regression model for urban land use land cover change analysis and its impact on land surface temperature in Jimma City, southwestern Ethiopia. Applied Geomatics, 1–15.

Mo, Y., Xu, Y., Chen, H., & Zhu, S. (2021). A review of reconstructing remotely sensed land surface temperature under cloudy conditions. Remote Sensing, 13(14), 2838.

Moazzam, M. F. U., Doh, Y. H., & Lee, B. G. (2022). Impact of urbanization on land surface temperature and surface urban heat island using optical remote sensing data: A case study of Jeju Island, Republic of Korea. Building and Environment, 222, 109368.

Mohammad, P., Goswami, A., & Bonafoni, S. (2019). The impact of the land cover dynamics on surface urban heat island variations in semi-arid cities: a case study in Ahmedabad City, India, using multi-sensor/source data. Sensors, 19(17), 3701.

Mundhe, N. N., & Jaybhaye, R. G. (2014). Impact of urbanization on land use/land covers change using Geo-spatial techniques. International Journal of Geomatics and Geosciences, 5(1), 50–60.

Mundia, C. N., & Aniya, M. (2020). Land-use and land cover change in Nairobi: Implications for sustainable urban planning. Environmental Management, 45(6), 897–911.

NASA Earth Observatory. (2010). Vegetation & Land Surface Temperature. Retrieved from https://earthobservatory.nasa.gov

Odindi, J. O., Bangamwabo, V., & Mutanga, O. (2015). Assessing the value of urban green spaces in mitigating multi-seasonal urban heat using MODIS land surface temperature (LST) and Landsat 8 data. International Journal of Environmental Research, 9, 9–18.

Pettorelli, N., Vik, J. O., Mysterud, A., Gaillard, J. M., Tucker, C. J., & Stenseth, N. C. (2005). Using the satellite-derived NDVI to assess ecological responses to environmental change. Trends in Ecology & Evolution, 20(9), 503–510.

Regassa, B., Kassaw, M., & Bagyaraj, M. (2020). Analysis of urban expansion and modeling of LULC changes using geospatial techniques: The case of Adama City. Remote Sensing of Land, 4(1-2), 40-58.

Roy, B., Kanga, S., & Singh, S. K. (2017). Assessment of land use/land cover changes using geospatial techniques at Osian-Mandore, Jodhpur (Rajasthan). International Journal of Scientific Research in Computer Science, Engineering and Information Technology, 2(5), 73–81.

Roza, A., Suryabhagavan, K. V., Balakrishnan, M., & Hameed, S. (2017). Geo-spatial approach for urban green space and environmental quality assessment: A case study in Addis Ababa City. Journal of Geographic Information System, 9, 191–206.

Sabr, A., Moeinaddini, M., & Azarnivand, H. (2016). Assessment of land use and land cover change using spatiotemporal analysis of landscape: Case study in south of Tehran. Environmental Monitoring and Assessment, 188(6), 691. https://doi.org/10.1007/s10661-016-5701-9

Saha, S., Saha, A., Das, M., Saha, A., Sarkar, R., & Das, A. (2021). Analyzing spatial relationship between land use/land cover (LULC) and land surface temperature (LST) of three urban agglomerations (UAs) of Eastern India. Remote Sensing Applications: Society and Environment, 22, 100507.

Sathianarayanan, M., & Hsu, P. H. (2019). Impact of urbanization on land surface temperature using deep learning approach. Urban Climate, 34, 100694.

Shahfahad, M., Khan, S. U., & Aziz, M. (2020). Influence of urbanization on land surface temperatures: The role of vegetation in mitigating heat islands. Urban Climate, 34, 100694.

Singh, R. B., Grover, A., & Zhan, J. (2014). Inter-seasonal variations of surface temperature in the urbanized environment of Delhi using Landsat thermal data. Energies, 7, 1811–1828.

Sruthi, S., & Mohammed, A. (2015). Agricultural drought analysis using the NDVI and land surface temperature data: A case study of Raichur District. Aquatic Procedia, 4, 1258–1264.

Sundarakumar, K., Harika, M., Begum, S. A., Yamini, S., & Balakrishna, K. (2012). Land use and land cover change detection and urban sprawl analysis of Vijayawada city using multitemporal Landsat data. International Journal of Engineering Science and Technology, 4(01), 170–178.

Taloor, A. K., Manhas, D. S., & Kothyari, G. C. (2021). Retrieval of land surface temperature, normalized difference moisture index, normalized difference water index of the Ravi basin using Landsat data. Applied Computing and Geosciences, 9, 100051.

Tan, J., Yu, D., Li, Q., Tan, X., & Zhou, W. (2020). Spatial relationship between land use/land cover changes and land surface temperature in the Dongting Lake area, China. Scientific Reports, 10(1), 1–9.

Terfa, B. K., Chen, N., Liu, D., Zhang, X., & Niyogi, D. (2019). Urban expansion in Ethiopia from 1987 to 2017: Characteristics, spatial patterns, and driving forces. Sustainability, 11(10), 2973.

Trigo, I. F., Monteiro, I. T., Olesen, F., & Kabsch, E. (2008). An assessment of remotely sensed land surface temperature. Journal of Geophysical Research: Atmospheres, 113(D17).

Uddin, M. J., & Swapnil, F. J. (2021). Land surface temperature (LST) estimation at Kushtia District, Bangladesh. Journal of Civil Engineering, Science and Technology, 12(2), 213–227.

Vancutsem, C., Ceccato, P., Dinku, T., & Connor, S. J. (2010). Evaluation of MODIS land surface temperature data to estimate air temperature in different ecosystems over Africa. Remote Sensing of Environment, 114(2), 449–465.

Walther, B. A., & Moore, J. L. (2005). The concepts of bias, precision and accuracy, and their use in testing the performance of species richness estimators, with a literature review of estimator performance. Ecography, 28(6), 815–829.

Wang, M., He, G., Zhang, Z., Wang, G., Wang, Z., Yin, R., & Cao, X. (2019). A radiance-based split-window algorithm for land surface temperature retrieval: Theory and application to MODIS data. International Journal of Applied Earth Observation and Geoinformation, 76, 204–217.

Wang, R., Hou, H., Murayama, Y., & Derdouri, A. (2020). Spatiotemporal analysis of land use/cover patterns and their relationship with land surface temperature in Nanjing, China. Remote Sensing, 12(3), 440.

Wang, S., Qifan, Y., Haiyoung, D., & Hanwei, L. (2016). Detection of urban expansion and land surface temperature change using multitemporal Landsat images. Resource Conservation and Recycling, 128, 526–534. https://doi.org/10.1016/j.resconrec.2016.05.011

Xu, H. (2008). A new index for delineating built-up land features in satellite imagery. International Journal of Remote Sensing, 29(14), 4269–4276. https://doi.org/10.1080/01431160801922968

Xu, H., Zhang, Y., & Li, J. (2023). Evaluating urban growth and environmental sustainability using the NDBI and NDVI indicators. International Journal of Remote Sensing, 44(5), 1183–1201.

Yin, C., Meng, F., & Yu, Q. (2020). Calculation of land surface emissivity and retrieval of land surface temperature based on a spectral mixing model. Infrared Physics and Technology, 108, 103333.

You, M., Lai, R., Lin, J., & Zhu, Z. (2021). Quantitative analysis of a spatial distribution and driving factors of the urban heat island effect: A case study of Fuzhou Central Area, China. International Journal of Environmental Research and Public Health, 18(24), 13088.

Zha, Y., Gao, J., & Ni, S. (2003). Use of the normalized difference built-up index in automatically mapping urban areas from TM imagery. International Journal of Remote Sensing, 24(3), 583–594.

Zhang, J., Jiao, G., Ye, Q., & Gu, X. (2022). The impact of urban expansion on the urban thermal environment: A case study in Nanchang, Jiangxi, China. Sustainability, 14(24), 16531.

Zhang, X., Friedl, M. A., Schaaf, C. B., Strahler, A. H., & Liu, Z. (2018). Monitoring the response of vegetation phenology to urbanization in the conterminous United States. Remote Sensing of Environment, 211, 154–166.

APPENDICES

Appendix 1. Landsat Images of the study area from 1990 to 2024.

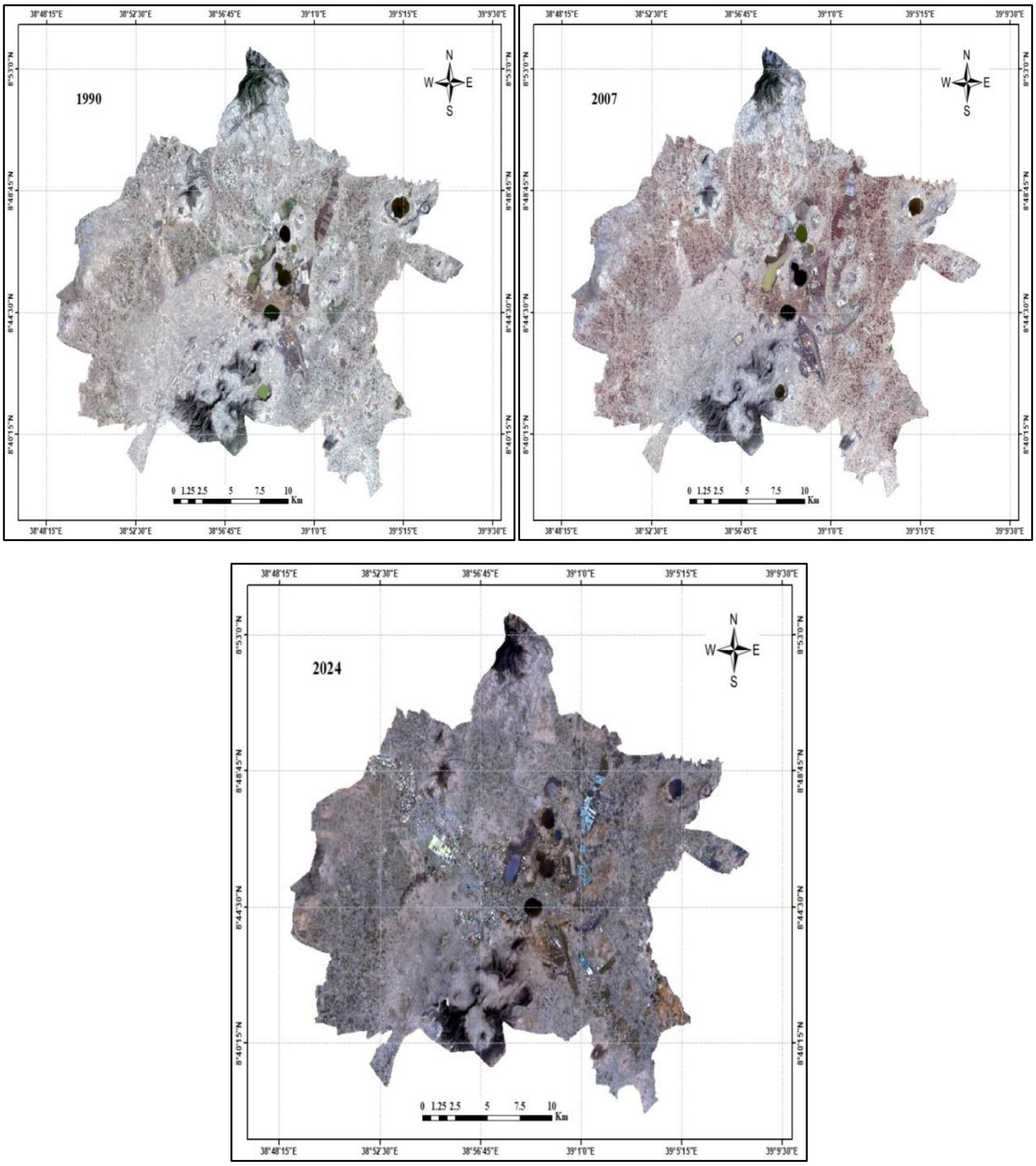

Appendix 2: Google earth image showing study area LULC

Appendix 3. Classification accuracy assessment report for the year 1990

Classes	Agriculture	Bare land	Built-up	Vegetation	Water	Row Total
Agriculture	77	1	1	1	0	80
Bare land	0	9	1	0	0	10
Built-up	1	0	58	1	0	60
Vegetation	3	0	2	34	1	40
Water	0	0	0	1	9	10
Column Total	81	10	62	37	10	200

Appendix 4. Classification accuracy assessment report for the year 2007

Classes	Agriculture	Bare land	Built-up	Vegetation	Water	Row Total
Agriculture	75	2	2	1	0	80
Bare land	0	9	1	0	0	10
Built-up	1	0	58	0	0	60
Vegetation	3	0	2	34	1	40
Water	0	0	0	1	9	10
Column Total	79	11	63	37	10	200

Appendix 5. Classification accuracy assessment report for the year 2024

Classes	Agriculture	Bare land	Built-up	Vegetation	Water	Row Total
Agriculture	78	1	0	1	0	80
Bare land	0	9	1	0	0	10
Built-up	1	0	58	0	0	60
Vegetation	2	0	2	35	1	40
Water	0	0	0	1	9	10
Column Total	81	10	61	38	10	200